OXIDATIVE COUPLING OF METHANE OVER LANTHANUM AND STRONTIUM PROMOTED MAGNESIUM CATALYST

by

Sezin SEZEN

B.S., Chemical Engineering, Istanbul University, 2010

Submitted to the Institute for Graduate Studies in
Science and Engineering in partial fulfillment of
the requirements for the degree of
Master of Science

Graduate Program in Chemical Engineering

Boğaziçi University

2014

to my precious family

ACKNOWLEDGEMENTS

Firstly, I would like to express my sincere thanks to my thesis supervisor Prof. Ramazan Yıldırım. His advices helped me to improve not only my work but also my life, and his guidance was invaluable throughout my thesis. It was a great honor for me to work with him during my graduate thesis. This thesis would not have been possible without his inspiration and effort.

I would like to express my gratitude also for my thesis committee members; Assoc. Prof. Ahmet Kerim Avcı and Assoc. Prof. Hasan Bedir.

First of my special thank goes to Yeşim Düşova Teke because of her endless patience to help my learning process whenever I need and her precious friendship during long working hours spending at laboratory 403 not only with her pleasant chitchat but also delicious meals.

At the same time, Aybüke Leba who has deserved an other special thanks from me specially for her endless patience. Most of the complicated problems could be easier thanks to her suggestions.

Of course, in this working process, concentrating was the most important part. Melek Selcen Başar and Elif Erdinç who help me to concentrate on thesis whenever I need, deserves of the best gratitude with their precious friendships.

It was an honour to work with CATREL team, especially A. İpek Paksoy, Merve Eropak, Ali Uzun, Cansu Yassı, Onur Kavaklı, Sinan Koç, Çağla Odabaşı, Özgür Yaşar Çağlar, Çiğdem Ekmen, Hazal Bal. Cordial thanks for Bilgi Dedeoğlu, Yakup Bal for their technical assistance, secretaries Melike Gürbüz.

I would like to thank to my friends in graduate class, Özge Ertem, Didem Büşra Kabakçı and at last especially, Büşra Gürses for her accompaniment in long working

hours. Whenever I need positive thinking, she help me with her endless life energy. I consider myself so lucky to have such a good friend.

At last but most importantly, I want to present my appreciation to my family, Fahreddin Sezen, Semiha Sezen and Gülce İzel Sezen that stand always behind me and encourage lifelong. If I had a chance to reborn and chose family from the beginning, I would choose them again and again. I have no word can describe precisely how they are precious for me.

The financial support for this thesis was provided by TÜBİTAK through project 112M714.

ABSTRACT

OXIDATIVE COUPLING OF METHANE OVER LANTHANUM AND STRONTIUM PROMOTED MAGNESIUM CATALYST

The oxidative coupling of methane (OCM) over 10wt.%SrO/10wt.%La_2O_3/MgO, in the form of particulate and monolithic structures, was investigated in this thesis. The OCM performance of the catalyst, which was prepared using incipient to wetness impregnation and then wall-coating over the monolithic support, was investigated in a microflow quartz reactor.. The diameter of reactor was 10 mm around the catalyst bed and reduced to 2 mm at the exit to decrease the void volume, which was also filled with quarts chips to prevent undesired gas phase reactions. At the beginning of work, 10wt.%La_2O_3/MgO particulate catalyst was prepared by incipient to wetness impregnation and tested. At the following stages, the additional metal oxides (CaO and SrO) were also added. The highest yield was 8wt.% in particulate catalysts and it was observed over 10wt.%SrO/10wt.% La_2O_3/MgO. For the test over mullite monolith, the monolith blocks were shaped to 17 mm height and 8 mm ID first, and then they were wash-coated with MgO followed by La_2O_3 and/or SrO. The highest C_2 yield (14.5%) was obtained at 650 ^oC with CH_4/O_2 ratio of 15 using 10wt.%SrO/10wt.% La_2O_3/MgO over monolith.

ÖZET

$SrO/La_2O_3/MgO$ KATALİZÖRÜ ÜZERİNDE METANIN OKSİJEN VARLIĞINDA YÜKSEK HİDROKARBONLU MOLEKÜLLERE DÖNÜŞÜMÜ

Bu tezde, metanın oksijen varlığında katalitik olarak etan ve etilene dönüştürülmesi (OCM) reaksiyonu, partikül ve monolit formundaki %10SrO/%10La_2O_3/MgO katalizörü kullanılarak incelenmiştir. Islak emdirme ve daldırarak kaplama yöntemleriyle hazırlanan katalizörünün OCM performansı mikro akışlı kuvars bir reaktör kullanılarak test edilmiştir. Katalizör yatağında 10 mm olan reaktör çapı boşluk hacmini azaltmak için çıkışta 2 mm'ye düşürülmüş, ilave olarak boşluk, kuvars parçalarıyla doldurularak istenmeyen gaz fazı reaksiyonları önlenmeye çalışılmıştır. Çalışmalara ıslak emdirme metoduyla hazırlanan partikül halindeki 10wt.%La_2O_3/MgO katalizörü ile başlanmış daha sonra farklı metal oksitlerin (CaO ve SrO) katkısı ile devam edilmiştir. Bunların arasında en yüksek verim %8 ile %10 SrO ve %10 La_20_3'in MgO üzerine eklenmesi ile elde edilen katalizörde elde edilmiştir. Mullite monolitle yapılan testlerde ise, monolit blok 17 mm yüksekliğinde ve 8 mm çapında parçalara kesilerek üzerine önce MgO, sonra da La_2O_3, SrO veya La_2O_3-SrO karışımı daldırma metodu ile kaplanmıştır. En yüksek C_2 verimi %14.5 olarak; 650 ^oC'de %10SrO/%10La_2O_3/MgO monolit katalizör üzerinde, CH_4/O_2 oranı 15 değerinde iken elde edilmiştir.

TABLE OF CONTENTS

LIST OF FIGURES

LIST OF TABLES

LIST OF SYMBOLS

χ_{CH_4}	Conversion of Methane
S_{C_2}	Selectivity of C_2
Y_{C_2}	Reaction Yield

LIST OF ACRONYMS/ABBREVIATIONS

F-T	Fischer Tropsch Process
DME	Dimethyl Ether
EDX	Energy Dispersive X-Ray Spectroscopy
ID	Inside Diameter
MSR	Microstructured Ether
OCM	Oxidative Coupling of Methane
SEM	Scanning Electron Microscope
SOM	Selective Oxidation of Methane to Formaldehyde and Methanol
XRD	X-ray Diffraction

1. INTRODUCTION

As petroleum reserves are dwindling around the world, conversion of natural gas into more useful chemicals and fuels is recognized as one of the next step to sustain economic growth and maintain fuel supplies (Lunsford, 2000; Bouwmeester, 2003). Considerable world-wide researches have been conducted to develop various commercially viable processes for methane conversion via the direct or indirect routes. Compared to the indirect conversion technologies that need the energy intensive step of syngas formation, the direct route that converts methane into higher hydrocarbons in one step, as the oxidative coupling reactions (OCM), is potentially more economically attractive and consequently has been intensively studied (Frade *et al.,* 2004).

In previous literature studies that assume lower oil prices, it has been estimated that a single-pass conversion of 35-37% and selectivity of 88-85%, equivalent to a C_2 yield of >30%, is required to attain commercial competitiveness for OCM (Tan *et. al.*, 2007). In fact, results obtained are still far away from this expectation while the limit of the C_2 yield in a fixed bed reactor is found to be around 25% (Olivier *et al.,* 2009). Despite extensive research efforts in the past, process concepts investigated mainly were fixed bed reactors. Thus, alternative reactor concepts with adapted catalysts have to be explored and eventually invented. One of the most promising design solutions could be the micro reactors with the capacity of better heat removal, hence the suppression of hot spot formation (Kolb *et al.*, 2004).

To date, various oxide catalysts have been researched. Basic oxides, such as alkali metal oxides, alkaline earth metal oxides, and rare earth oxides, show high C_2 selectivity in the OCM reaction; especially, La_2O_3 and SrO are well-known effective catalysts. Additionally, it has a high stability and activity. So in presence work, La_2O_3 and SrO promoted MgO will be used as the catalyst.

The purpose of this research was to prepare La_2O_3 and/or SrO catalysts over MgO support coated in a mullite monolith, and compare the results with the results over particulate catalyst under the same temperature and feed conditions. It was also aimed to

determine the most suitable conditions for high C_2 hydrocarbon yield over micro structured reactors. The best performing catalysts were also characterized using the methods like SEM, XRD and EDX.

Chapter 2 contains the literature survey on oxidative coupling of methane process, catalysts, influence of the operating conditions (feed gas composition, temperature and pressure), reactor types and methods for catalyst preparation. In Chapter 3, experimental system and catalyst preparation methods will be explained. The experimental results will be shown and discussed in Chapter 4 and finally the conclusion of the study and recommendation will be summarized in Chapter 5.

2. LITERATURE SURVEY

Methane is the principal component of most natural gas reserves that is currently used for home and industrial heating. A number of strategies ranging from fundamental science to engineering technology are being explored to utilize methane more effectively. In the following part, various ways of methane utilization will be summarized.

2.1. Methane Utilization

In many respects, methane is an ideal fuel for home and industrial heating as well as for the generation of electrical power because of its availability in most populated centers, and its ease of purification to remove sulfur compounds. It has the largest heat of combustion relative to the amount of CO_2 formed (Lunsford, 2000).

The utilization rate of methane is near to 1.7×10^9 tons of oil equivalent per year (Fujimoto *et al.*, 1994). The reserves of natural gas exceed that of oil by about 50%, the rate of discovery of new reserves of natural gas also outstrips the rate of discovery of oil reserves (Zhu *et al.*, 2004).

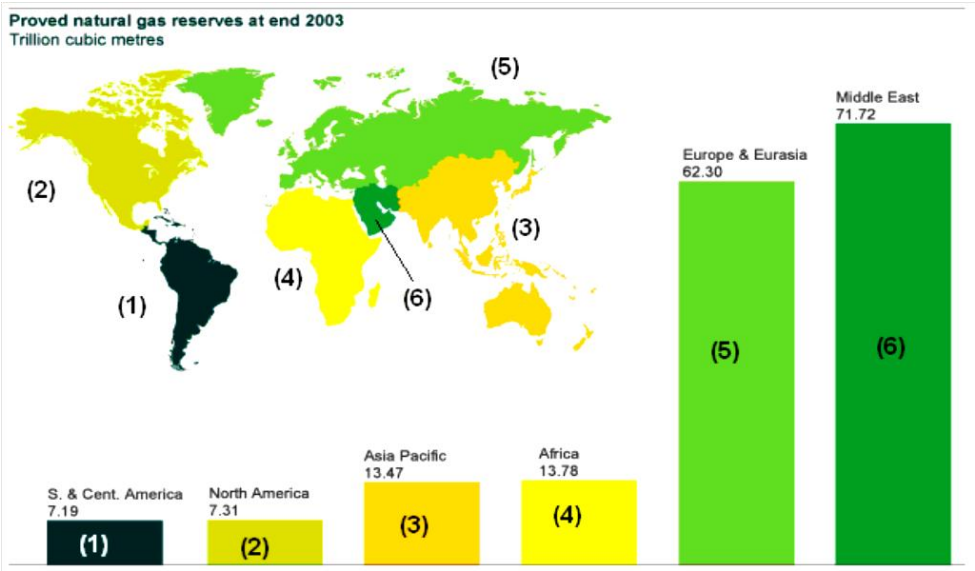

Figure 2.1. Geographical Distribution of Natural Gas Reserves (Jianjun Zhu *et al.*, 2004).

Much of the methane is found in regions that are far removed from industrial complexes and often it is produced off shore (Figure 2.1). Pipelines may not be available for transporting this remote gas to potential markets and liquefaction for shipping by ocean-going vessels is expensive. Strategies for the use of methane depend on its price and location, the demand for products, construction costs, the economic and political stability of a region and many other factors (Lunsford, 2000).

2.2. Methane Utilization Methods

Since there are enormous proven reserves of natural gas in the world, there is a strong economic incentive to develop a process that would convert methane into more valuable chemicals and fuels.

Considerable world-wide researches have been conducted to develop various commercially viable processes for methane conversion via the direct or indirect routes as shown in Figure 2.2.

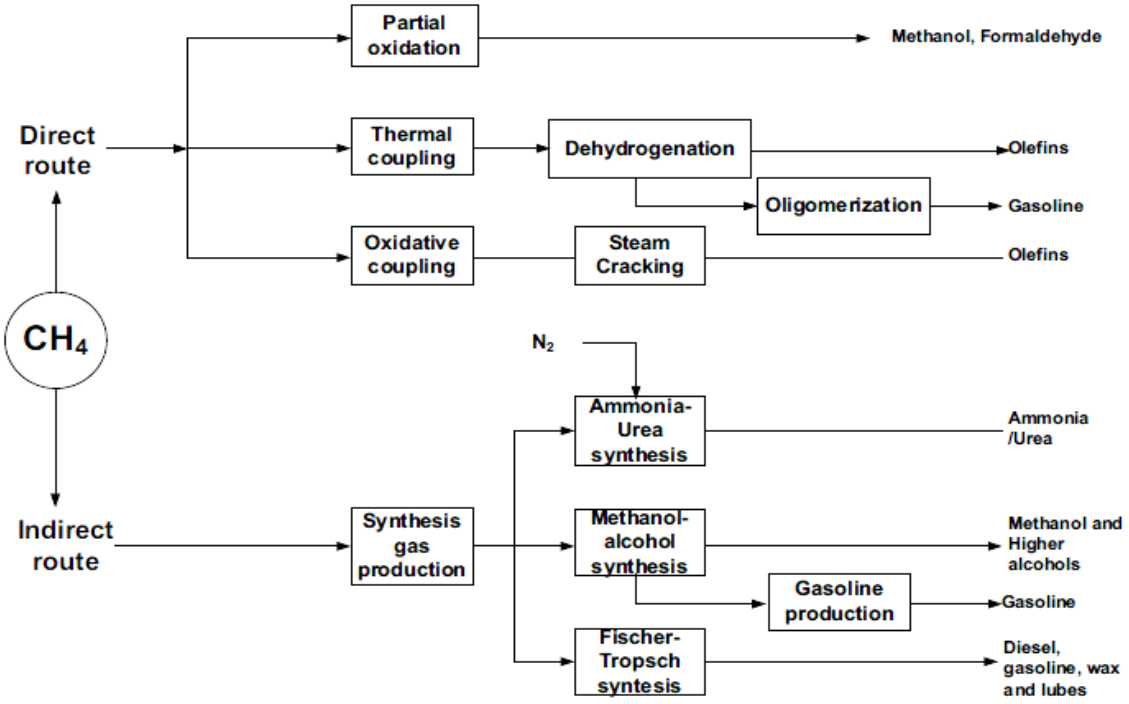

Figure 2.2. Conceptual Routes for Chemical Conversion of Methane (Zhu *et al.*, 2004).

2.2.1. Indirect Utilization of Methane

The indirect route is a two-step process whereby natural gas is first converted to synthesis gas (a mixture of H_2, and CO) via steam reforming, partial oxidation, CO_2 reforming or combination of three reactions. In the second step, synthesis gas is converted to the desired products in downstream processes such as methanol production, ammonia synthesis and Fischer-Tropsch synthesis. The most important reactions in syngas production step are:

Steam reforming	: $CH_4 + H_2O \leftrightarrow CO + 3H_2$	($\Delta H^\circ_{298\ K}$ = 206 kJ/mol)	(2.1)
CO_2 reforming	: $CH_4 + CO_2 \leftrightarrow 2CO + 2H_2$	($\Delta H^\circ_{298\ K}$ = 247 kJ/mol)	(2.2)
Partial oxidation	: $CH_4 + ½O_2 \leftrightarrow CO + 2H_2$	($\Delta H^\circ_{298\ K}$ = -35 kJ/mol)	(2.3)
Water gas shift reaction	: $CO + H_2O \leftrightarrow CO_2 + H_2$	($\Delta H^\circ_{298\ K}$ = -41 kJ/mol)	(2.4)

Two major important processes, which utilize natural gas via synthesis gas, are methanol synthesis and Fischer-Tropsch (Zhu *et al*., 2004).

2.2.1.1. Methanol Synthesis. Synthesis gas is primarily used for the production of methanol, a starting point of the route to dimethyl ether (DME), gasoline and ethylene. Thermodynamically, this process is favored by a decrease in temperature, which would shift the equilibrium towards the formation of methanol (Rozovskii *et al.,* 1975). Initially zinc-chromium oxide catalysts requiring relatively high temperatures and high pressures were used for this purpose. Then more active copper-zinc-aluminum catalysts were discovered and this made it possible to conduct the process at lower temperatures and pressures. However paradoxically, formation of intermediate CO_2 takes place over the copper-containing catalysts and reduces the methanol production. Therefore, the initial reaction mixture in the "low pressure" process must contain a certain amount of CO_2 (Zhu *et al*., 2004).

2.2.1.2. Fischer-Tropsch Process. Another important development in the use of synthesis gas is the Fischer-Tropsch (F-T) process, which has a long history (Dry, 2002). Over Fe, Co, Ru or similar metals, synthesis gas can be converted to paraffinic liquid fuels through F-T reactions:

$$nCO + 2nH_2 \rightarrow (-CH_2)n + nH_2O \quad (2.5)$$

Current commercial F-T reactors operate in two different temperature ranges. The high temperature F-T operates with iron catalysts at about 340 °C and is geared mainly at the production of olefins and gasoline. The low temperature F-T, using either iron or cobalt based catalysts at about 230 °C, is geared at the production of diesel and linear waxes.

The expected future trend towards non-petroleum sources of fuel and, in particular, plenty of methane reserves provide a strong stimulus for the further development of the process on the basis of new fundamental knowledge (Rozovskii *et al.,* 1975).

2.2.2. Direct Utilization of Methane

The direct routes are one-step processes in which the natural gas is directly converted to desired products. Compared with the indirect methods, direct methods are potentially simpler in technology and more economical. However, apart from complete combustion for heating purposes (giving CO_2, and water), all other direct conversion routes have not yet been realized on industrial scale. This is mostly because conversions and selectivity are not sufficiently high to be of interest for commercial application. Two major direct conversion routes are oxidative coupling of CH_4 to C_2 hydrocarbons (OCM) and partial oxidation of CH_4 to formaldehyde and methanol (SOM) (Pyatnitskii *et al.,* 2003).

2.2.2.1. Oxidative Coupling of Methane to Higher Hydrocarbons. The heterogeneously catalyzed OCM seems to be one of the most promising routes to convert methane directly from the abundant natural gas into ethylene which is a feed-stock for chemical industry, and by oligomerization of ethylene into transportation fuels.

Two factors handicap commercialization of this process:

(i) C_2 selectivity and yield are too low and
(ii) Technological novelty results in uncertainty for scale-up.

Higher C_2 selectivity and yield have to be achieved through development of more selective catalysts; but optimization of reaction conditions, reactor design and operation

also offer possibilities to improve catalytic performance. The technological uncertainty is due to the fact that all results available until now have been achieved in laboratory-scale units, mainly in microcatalytic fixed-bed and small-scale fluidized-bed reactors.

Due to the complexity of the OCM reaction, scale-up can be associated with a loss in catalytic performance. Moreover, the severe reaction conditions, i.e. high temperature and exothermicity require new reactor designs. Therefore, experience from other selective oxidation reactions can be used only to a limited extent.

Reactor development includes not only choice of the reactor type but also selection of materials and the method of temperature control; the reaction engineering aspects of the OCM reaction play an important in the attempt to make this process commercially viable (Mleczko *et al.*, 1994).

C_2H_6 is the primary product while C_2H_4 is also a desirable secondary product. The catalyst is activated through dissociative oxygen chemisorption and subsequently produces gas phase methyl radicals by hydrogen abstraction from methane (Figure 2.3). Methyl radicals can couple in the gas phase to form ethane, which in turn can be dehydrogenated into ethylene. However, they can also be oxidized toward undesired carbon oxides, CO and CO_2 in the gas phase as well as by interaction with the catalyst surface (Chen *et al.*, 1991).

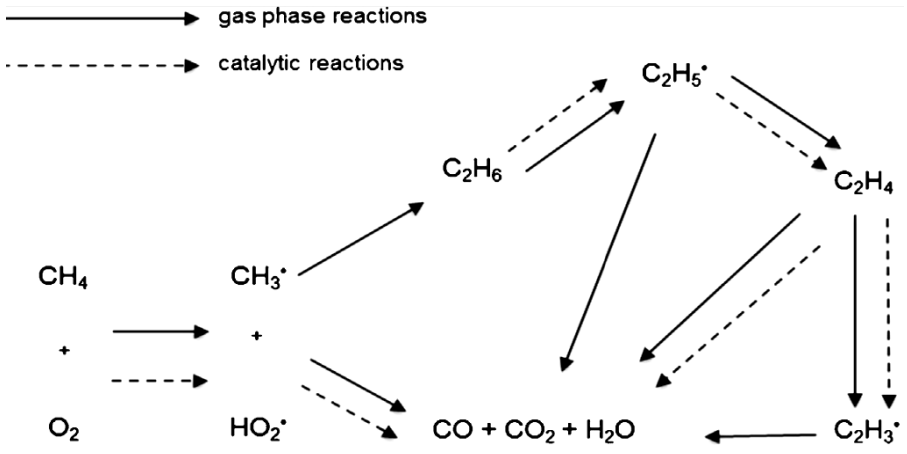

Figure 2.3. Reaction Steps Involved in OCM Reaction (Chen *et al.*, 1991).

The OCM process also involves some other reactions of CH_4, O_2 and the products; the major reactions are listed below (Lunsford, 2000).

(1) $CH_4 + 2O_2 \rightarrow CO_2 + 2H_2O$ (2.6)

(2) $2CH_4 + ½O_2 \rightarrow C_2H_6 + H_2O$ (2.7)

(3) $CH_4 + O_2 \rightarrow CO + 2H_2O$ (2.8)

(4) $CO + 1/2\,O_2 \rightarrow CO_2$ (2.9)

(5) $C_2H_6 + ½\,O_2 \rightarrow C_2H_4 + H_2O$ (2.10)

(6) $C_2H_4 + 2O_2 \rightarrow 2\,CO + 2H_2O$ (2.11)

(7) $C_2H_4 + 2H_2O \rightarrow 2\,CO + 4H_2$ (2.12)

(8) $C_2H_6 \rightarrow C_2H_4 + H_2$ (2.13)

(9/10) $CO + H_2O \leftrightarrows CO_2 + H_2$ (2.14)

2.2.2.2. Selective Oxidation of Methane to Formaldehyde and Methanol (SOM). Partial oxidation of methane to methanol may have high selectivity (about 80%) under optimal conditions, but the yield of methanol per pass is still less than 7% due to very low CH4 conversion for a single pass. This results in requirement for a very big recycle ratio and difficulty in product separation due to low partial pressure of methanol. For comparison, commercial methanol production via synthesis gas route has typically a conversion per pass of 50%, and only a recycle ratio of four is required. Selectivity to methanol is above 99% (Zhu *et al*., 2004).

$$CH_4 + ½\,O_2 \rightarrow CH_3OH \quad (2.15)$$

2.3. Catalysts for Oxidative Coupling of Methane

A large number of compounds have been tried as the catalysts for the oxidative coupling of methane, and it is impossible to classify those materials unambiguously into distinct groups. Nevertheless, they are divided here into three major groups by periodic table location as a matter of convenience:

(i) alkali and alkaline earth metal compounds;
(ii) the compounds of lanthanide and actinide metals; and
(iii) other metal compounds.

The third group may be further divided into the compounds of transition metals and those of post transition metals.

Since Lunsford and his co-workers (1999) first demonstrated that lithium-doped magnesia was an active and selective catalyst for the oxidative coupling reaction, alkali metal-doped alkaline earth metal oxide catalysts have been studied by many workers. These catalysts are often called alkali-promoted magnesia, alkali-promoted calcium oxide, and so on. However, the active centers of a Li/MgO catalyst, for example, were found to be the surface Li^+ - O^- species, as discussed later. Hence it seems, to be more appropriate to call it magnesia-supported lithium oxide catalyst. Nonetheless, the terms promoter and support are used conventionally in this review since the active centers are not always identified (Ito *et al.*, 1985).

Keller and Bhasin found that many metal oxides showed activity for the coupling reaction. Generally, metals in the most active group have multiple oxidation states and most of them belong to the low melting metal part of the periodic table (Keller *et al.*, 1982).

2.3.1. The Alkali and Alkaline Earth Metals

Alkali-doped alkaline earth metal oxides have been studied by many investigators. Both alkaline earth (Mg, Ca, Sr, and Ba) and rare earth (La, Ce, Nd, Sm, Gd, Er and Yb) metals play crucial roles in determining the surface properties (basicity/base strength distribution and acidity/acid strength distribution) and activity of the supported catalyst in the process (Choudhary *et al.,* 1999). According to Choudhary and Uphade (2004), the performance of alkali earth metal and promoted rare earth oxide catalysts can be improved by adding an alkaline earth promoter. It is found that the unsupported catalyst such as Nd_2O_3, Eu_2O_3 and La_2O_3 has a better activity and selectivity with the strong basic sites of La and Nd oxides to develop catalytic activity. It is indicated by Choudhary and Uphade (2004) that the Sr promoted La_2O_3 showed the best performance.

Doping with a proper alkali metal, however, increases the conversion and selectivity significantly. A combination of lithium and magnesia is the most frequently used doped system for this purpose (Fujimoto *et al.,* 1987).

Although they are less selective than optimum Li systems, other alkali metals have also been shown to be highly effective in promoting MgO. For Na/MgO, up to 22.4% C_2 yields have been published at literature (Iwamatsu *et al.,* 1987) The combination of Li and lanthanide (La. Ce, Nd, or Sr) promoters for MgO gives spectacular selectivity to C_2 (98.4%) at conversions to 25%, and the catalysts are stable to time on stream of 2.5-10 (Ghiasi *et al.,* 2011).

Other alkaline earth oxides, Group 3 metal, transition metal, or post transition metal oxides, as supports or promoters, do not seem to be as effective as Li in promoting MgO, with the notable exceptions of Mn/MgO promoted with Na (Labinger *et al.,* 1990) and a mixed PbO-MgO catalyst (Bartek *et al.,* 1988).

The alkaline earth oxides, including MgO, have received wide attention as basic supports with promotion by alkali metals. Although calcium oxide is less studied compared with magnesium, it is also an effective catalyst, especially promoted with alkali metals (Carreiro *et al.,* 1988). In general, catalysts comprising alkali metal salts on CaO are of low surface area. The effectiveness and product distribution (ethane, ethylene, C_{3+}, CO_x)

vary with both the alkali metal and the anion, but not over a wide range of values. Addition of lanthanum to Na_2O/CaO does not have a significant effect. CaO doped with magnesium or calcium is also an effective catalyst (Fujimoto *et al.*, 1987).

Similarly, SrO and $SrCO_3$ have been used effectively both alone and promoted with alkali metal. Interesting systems, effective at high methane conversions, are the mixed oxides of Sr, Ce, Ce, and Yb. The effectiveness of these systems suggests that benefits may be obtained from studies of other mixed metal oxides of alkaline earths (Carreiro *et al.*, 1988; Machida *et al.*, 1987).

2.3.2. Lanthanide and Actinide Metal Oxide

The promoted lanthanide oxides seem to be the most promising catalysts so far for methane coupling. Not only the activity and selectivity, but also the catalyst life is a very important asset for the coupling catalysts under the severe reaction conditions employed. Compounds other than "simple" oxides, stable at coupling conditions, are clearly a prospect. High thermal stability and high productivity of La_2O_3 promoted by strontium attract some attention and become an interesting study.

Promotion of La_2O_3 with alkali or, especially, alkaline earth metals improves selectivity to C_2 (Burch *et al.*, 1988). The selectivity to C_2 over La_2O_3 is very high at low partial pressures of oxygen, but decreases with increasing O_2/CH_4 ratio. High selectivity to ethylene is attainable at low conversion. Ethane formed, or added to the feed stream, was converted both to ethylene and CO_2 (Otsuka *et al.*, 1986).

Choudhary and coworkers (Choudhary *et al.*, 1988) tested most of the lanthanum oxides, which included La, Ce, Pr, Nd, Sm, Eu, Gd, Dy, Er, Yb, as well as their strontium doped counterparts for the OCM reaction. The results showed that La_2O_3 and Sm_2O_3 are the most active non-doped catalysts and the doping by strontium improves the performance of all catalysts. For the strontium doped catalysts, the performance order of the base metal was found to be: La > Nd ≈ Sm ≈ Eu > Er ≈ Gd > Yb >> Pr ≈ Ce ≈ Dy.

Since lanthanum is a catalyst with high activity, this rare metal promised a lot of attention. The researches worked on Sr and Zn improves the selectivity while Ti and Nb

achieve the opposite result. The results also indicated that the selectivity improvement is related to the higher oxygen-anion conductivity achieved by Sr and Zn doping since the higher oxygen-anion conductivity favors the adsorption of gaseous oxygen and suppresses the non-selective reaction (Borchert *et al.,* 1997).

2.3.3. Transition and Post-Transition Metals

The majority of the catalysts in this group are based on mixed or supported metal oxides. Transition metal oxides are effective for OCM, when they are supported or promoted with alkali metals. Combination of Group V metals of the Periodic Table (vanadium, niobium and tantalum) with Group I metals as a binary and ternary metal oxide catalyst remarkably increase the catalytic performance.

Lead is one of the mostly studied transition metals. The conducted tests showed that, $PbMoO_4$, $PbWO_4$ and $PbCrO_4$, which have high oxygen anion mobility, showed very low C_2 selectivity (<20%) (Carreiro *et al.*, 1987).

Another research on lead was conducted by Hinsen and coworkers which tested different weight percentages of PbO supported on γ-alumina. These researches emerged that γ-alumina favors non-selective oxidation but the addition of PbO increases the C_2 selectivity up to 57.7%. Also, the addition of Na_2O to 6.5wt.% PbO/ γ -alumina increased the selectivity from 12.9% to 35.4%. This may cause since the addition of PbO or Na_2O decreases the acidity of the γ-alumina. This result observed in the C_2 selectivity increasing (Hinsen *et al.,* 1984).

The addition of alkali metals or metal salts to other transition metals was reported at Jones and coworkers' paper related with doped different metals (e.g. Na, Li, K, Rb, Cs, Mg, Ca, Ba, La) on 10% Mn/SiO_2, and found that sodium shows the best conversion and selectivity. The results also showed that the sodium source is an important factor in determining the improvement. The use of sodium pyrophosphate instead of sodium acetate increased the C_2 yield from 8.1% to 16.9%. The researchers also stated that the improvement is due to a combination of increased surface basicity, interaction between sodium and manganese, and a reduction of surface areas (Jones *et al*., 1987).

Using zinc oxide on different supports such as α-alumina, γ -alumina, and silica showed that both bulk and supported zinc oxide give low methane conversion activity (~20%) and low C_2 selectivity (<26% except α -alumina). However, the addition of any alkali metal chloride (Na, Li, or K) increased both conversion and selectivity, which increased the C_{2+} yield to 22.9% (Kim *et al*., 1995).

2.4. Effects of Operating Conditions on OCM Reaction

2.4.1. Partial Pressure of Reactants

The partial pressure of oxygen (CH_4/O_2 > 2-3) limits methane conversion due to stoichiometry of reaction. It also determines selectivity and therefore the amount of heat released. Low oxygen, high methane partial pressures promote high C_2 selectivity (Baerns *et al.*, 1990; Amenomiya *et al.*, 1990).

Since the low ratios of methane to oxygen partial pressures are necessary in order to achieve high degrees of methane conversion, the dependence of C_2 yield on the partial pressures of reactants follows that of methane conversion: the highest C_2 yields are achieved at highest conversion of methane but not at the highest C_2 selectivity. The drop of selectivity with increasing methane conversion is a fundamental obstacle to make the OCM commercially viable (Mleczko *et al.*, 1995).

2.4.2. The Effect of Reaction Temperature

The influence of temperature on C_2 selectivity is similar for all investigated catalysts. With increasing temperature, selectivity as well as yield pass through a maximum or reach a plateau. The temperature of maximum selectivity is specific for each catalyst and depends on the partial pressures of reactants as well as on mixing patterns which are different in various reactor types.

With increasing partial pressure of oxygen, the temperature of maximum C_2 selectivity is shifted to higher values. The increase in selectivity with growing temperature results from the higher activation energy of the selective primary reaction step compared to

the non-selective ones. Therefore, production of C_2 hydrocarbons increases stronger with temperature than of CO_x (Lin *et al*., 1988).

Lin and coworkers brought to attention that the formation of C_2 hydrocarbons is of second order for CH_3^* radicals although that of CO_x is of first order. When the rate of CH_3^* radical production increases at higher temperatures, relatively more C_2 hydrocarbons than CO_x, are formed compared to lower temperatures. The decrease of selectivity at high temperatures is caused by consecutive reactions which occur also in the gas phase. When complete conversion of oxygen is realized, the increasing C_2 selectivity is accompanied by an increase in methane conversion. This effect results from the stoichiometry of the OCM reaction; the selective reaction consumes less oxygen than the oxidation to CO_x. When a decrease of selectivity at high temperatures was caused by oxidation of C_2 hydrocarbons, this decrease was associated by a decrease of methane conversion for stoichiometric reasons (Andorf *et al*., 1991). However, when the drop of selectivity beyond the maximum was caused by steam reforming reactions, a continuous increase of methane conversion with temperature was illustrated (Mleczko *et al*., 1995).

2.4.3. The Effect of Reactor Pressure

The effect of total pressure is particularly important because it will be a major factor in determining the reactor size and the duty of compressors in the separation section. At elevated pressures and at conditions required for high CH_4 conversions, the extent of gas-phase reactions is substantial, even when the empty reactor is filled with an inert material.

In an empty reactor and for a given conversion, pressure does not influence C_2 selectivity (Wolf, 1992). OCM can be carried out at moderate pressure ($p < 0.3$MPa) without loss in product selectivity by appropriate adjustment in operating conditions. This conclusion is also confirmed by results obtained for the PbO/Al_2O_3 catalyst (Zanthoff, 1991). When applying pressures of 0.1 and 0.4 MPa, the highest C_2 selectivity was achieved as can be seen at Figure 2.4.

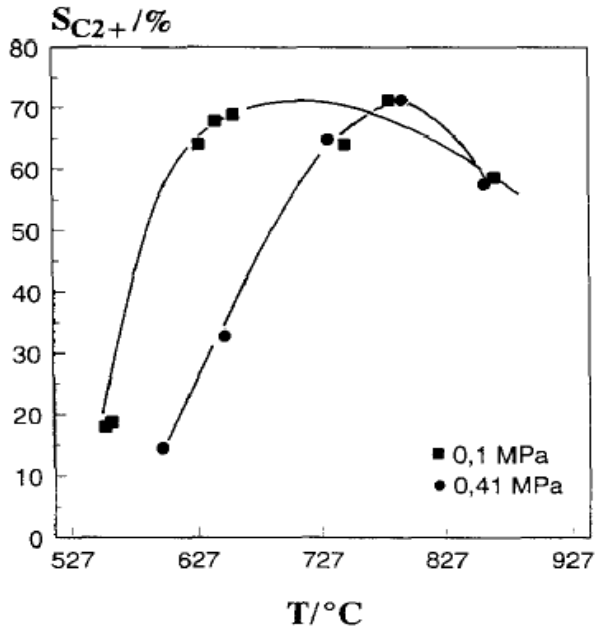

Figure 2.4. Effect of Temperature on C_2 Selectivity for the PbO/Al_2O_3 Catalyst Measured in a Fixed-Bed Reactor at 0.1 and 0.4 MPa Total Pressure. Reaction Conditions: CCH_4 = 67%, CO_2 = 7%, X_{O2} > 90% (Zanthoff, 1991).

2.5. Reactor Types Used for Oxidative Coupling of Methane Reaction

Since the OCM reaction comprises a complex reaction network it is obvious that selectivity and yield to C_2 hydrocarbons do not only depend on the catalyst but also on the type of reactor and reaction conditions. Various reactors have been considered: fixed beds, fluidized beds, membrane reactors, reactors with molten salts, reverse-flow reactors and countercurrent moving-bed reactors. Research and development work, however, was carried out mainly in catalytic fixed-bed and fluidized-bed reactors which both have a potential to be put into practice. For these reactor types also reaction engineering models were developed (Mleczko *et al.*, 1995).

The high exothermicity of the OCM reaction and the high activity of most catalysts resulted in various suggestions for novel designs of fixed-bed reactors, e.g. thin-bed reactor, sintered metal packing and monolithic reactor (Aigler *et al.*, 1991). The most important issue in OCM process is the formation of hot spots in the catalytic fixed bed reactor which causes undesired side reactions and catalyst deactivation; for this reason the

reactor concept, which does not allow effective heat management in exothermic reactions, is not suitable for this purpose.

The membrane reactors are also among the current investigation topics which in the reaction occur with oxygen on the catalyst lattice so the contribution of the gas-phase oxygen is mentioned as a deterministic factor to selectivity. This reactor design is pioneering to minimize the gas phase oxygen concentration in the reactor (Talebizadeh *et al*., 2009). Although this reactor type enables to perform the OCM reaction at very low oxygen concentration, no data confirming its feasibility for scale-up application were reported. Engineering problems like mechanical stability of membranes and temperature control in the reactor are still to be solved.

2.5.1. Microstructured Reactor (MSR)

There are several advantages of micro-structured reactors (MSR). Firstly, enhanced heat transfer is observed, which may be exploited for highly exothermic reactions due to the removal of the heat generated and the suppression of hot spot formation. Another aspect is the optimization of slow reactions getting close to the thermodynamic equilibrium (Gunther *et al*., 2004).

The high overall heat of the oxidative coupling of methane reaction causes hot spots (Arndt *et al*., 2011). Any excessive hotspots within the reactor as well as transport limitations should be avoided since selectivity is negatively affected (Choudhary *et al*., 1989). These negative effects can be minimized using MSR. Since they are suitable for fast, highly exothermic or endothermic chemical reactions because they lead to:

- process intensification,
- inherent reactor safety,
- broader reaction conditions including up-to the explosion regime,
- distributed production,
- faster process development (Renken *et al.*, 2005).

Process parameters such as pressure, temperature, residence time, and flow rate are more easily controlled in reactions that take place in small volumes. The hazard potential of strongly exothermic or explosive reactions can also be severely reduced (Veser, 2001).

Due to the properties mentioned above, microstructured reactors can be advantageously used as process engineering tools for acquiring information, which allows, in a short time and with greater safety, a process to be transferred to the pilot and production scale (Wörz *et al*., 2001).

Microstructured reactors also give opportunities for new production concepts. Depending on demand, more microstructured reactors or such subunits could be connected in parallel "numbering-up" so that the required intermediate products and end-products can be produced in their required amounts (Jähnisch *et al*., 2004).

The volumes of micro-reactors are still too large in order to interact with reactants significantly on a molecular level. Their main impact focuses on intensifying mass and heat transport as well as improving flow patterns. Therefore, benefits concerning chemical engineering aspects are the main driver for micro-reactor investigations, while chemistry remains unchanged in terms of reaction mechanism and kinetics. It is possible to present the advantages of the micro-structured reactors in terms of advantages arising from the decrease in the size and the increase in the number of units (Simsek, 2012).

2.5.2. Monolithic Reactors

Most monolith reactors consist of one piece of ceramic material. This ceramic block contains a large number of parallel channels extending over the entire length of the block, separated by thin walls. The channels usually have a small diameter, resulting in large specific surface areas, combined with the pressure drop. Various channel geometries exist: square, hexagonal, triangular, finned channels as seen at Figure 2.5, but also channel geometries produced by wrapping up flat sheets with corrugated sheets in between.

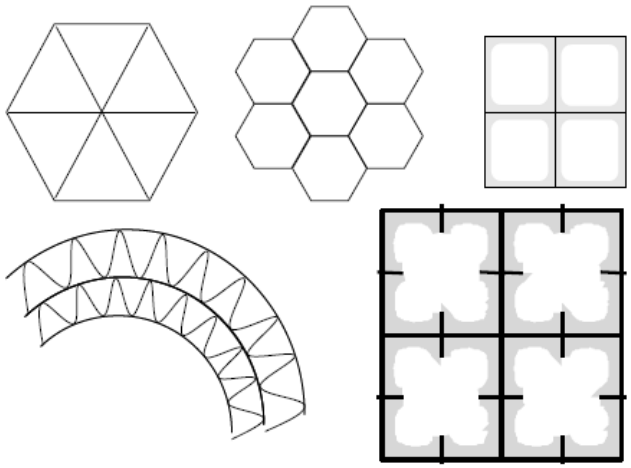

Figure 2.5. Various Channel Geometries of Monoliths (Düşova, 2014).

The monolith reactor was developed for the cleaning of exhaust gases from combustion processes, both in cars and large power plants. For these processes, the monolith reactor offers an irresistible combination of low pressure drop (two to three orders of magnitude lower than in packed beds) and high surface area (Moulijn *et al.*, 1998). The most important features of the monoliths are:

- Very low pressure drop in single and two-phase flow, one to two orders of magnitude lower than that of conventional packed bed systems,
- High geometrical areas per reactor volume, typically 1.5-4 times more than in the reactors with particulate catalysts,
- High catalytic efficiency due to very short diffusion paths in the thin wash coat layer,
- Exceptionally good performance in processes in which selectivity is hampered by mass-transfer resistances (Stankiewicz *et al.*, 2000).

One of the problems in monolith reactors, especially for gas-phase catalytic processes, is difficult heat removal due to the absence of radial dispersion. Monolith channels are fully separated from each other and, therefore, the only heat transport mechanism is the conductivity through the monolith material (Phillips *et al.*, 1997).

2.6. Methods for Catalyst Preparation

Methods of catalyst preparation are very diverse and each catalyst may be produced via different routes. Preparation usually involves several steps. Many supported metal and oxide catalysts are prepared by the succession of impregnation, drying, calcination, activation; zeolite catalysis are prepared by precipitation of gel, crystallization, washing, ion exchange, drying. Three fundamental stages of catalyst preparation may be distinguished:

- Preparation of the primary solid (or first precursory solid) associating all the useful components (e.g., impregnation or coprecipitation, or, in the case of zeolites, crystallization),
- Processing of that primary solid to obtain the catalyst precursor, for example by heat treatment,
- Activation of the precursor to give the active catalyst.

2.6.1. Impregnation Method

Impregnation consists of contacting a solid with a liquid containing the components to be deposited on the surface. In this work, incipient wetness impregnation method is applied. The required amounts of components are introduced in the volume corresponding to the pore volume of the support. The method is best suited to deposition of species which interact very weakly with the surface, and for deposition of quantities exceeding the number of adsorption sites on the surface (Haber *et al*., 1995). The most important part of this process, determining the volume of the solution corresponds to that beyond which the catalyst begins to look wet.

2.6.2. Monolithic Catalyst Preparation

The bare monoliths have a low surface area (generally 0.7 m^2/g for cordierite) (Özdemir, 2009) that is not suitable for the catalytic application. The active phase is needed to be deposited on the walls or inside the walls of inert monolith to increase the surface area. If the monolith structure is available in the required support material, the catalytically active phase can be directly deposited on the monolith. However, if the

monolith is not available in the required support material then this support material should be coated on the monolithic substrate first. The process is called as wash-coating (Figure 2.6).

Monolith structure can be coated via different techniques; with colloidal solution of the appropriate support in the form of suspended particles, with sol–gel method (the support is in the liquid phase) and with adequate suspensions and other procedures (Tomašić *et al.*, 2006).

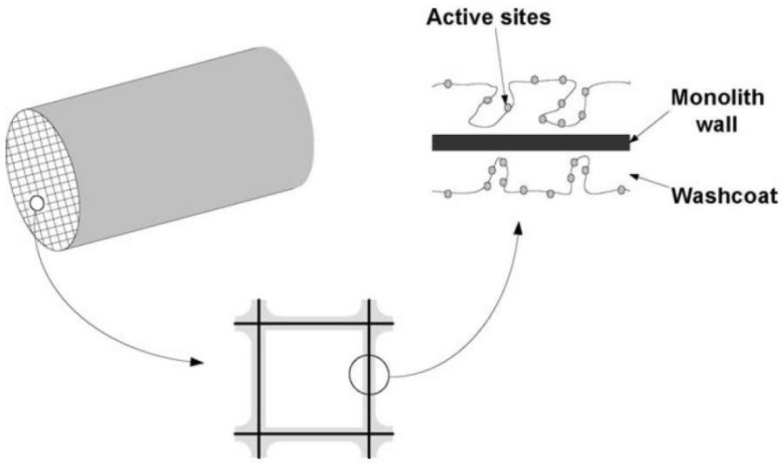

Figure 2.6. Schematic Diagram of a Monolith Structure (Tomašić *et al.*, 2006).

The most important parts of the coating procedure are loading of active phase onto monolith structure and homogenous dispersion of it. In the wash-coat method, firstly, the channels are wetted and filled with the coating solution and then, the channels are brandished by air through them. Following step is drying and calcination of the monolithic structure. The drying process is implemented via microwave.

3. EXPERIMENTAL WORK

3.1. Materials

3.1.1. Chemicals

All chemicals used for catalyst preparation are represented in Table 3.1.

Table 3.1. Chemicals used in catalyst preparation.

Chemicals	**Formula**	**Source**	**Molecular Weight (g/mol)**
Strontium Oxide	SrO	Aldrich	103.619
Strontium Nitrate	$Sr(NO_3)_2$	Merck	211.63
Lanthanum(III) Nitrate Hexahydrate	$LaN_3O_9 . 6H_2O$	Sigma Aldrich	433.01
Lanthanum(III) Oxide	La_2O_3	Sigma Aldrich	325.81
Calcium Oxide	CaO	Sigma Aldrich	63.01
Magnesium Oxide	MgO	Aldrich	56.08

3.1.2. Gases

The gases used in this study were listed with their specifications and applications in the Table 3.2.

Table 3.2. Applications and specifications of the gases used.

Gas	Specification	Application
Helium	99.998%	Inert, GC Carrier Gas
Methane	99.995%	Reactant
Oxygen	99.999%	Reactant

3.2. Experimental Systems

The experimental systems used may be divided into three groups:

(i) Catalyst Preparation Systems: The catalysts were prepared in various methods; incipient-to-wetness impregnation of active metals and coating of the cordierite monolithic support with active metals.

(ii) Catalytic Reaction System: System which is used for determining the catalytic activity of the catalysts consists of tubing, gas flow controller box, reactor, furnace, temperature controller, feed and product sampling sections and cold trap.

(iii) Product Analysis System: It consists of a gas sampling section, a gas chromatograph and a computer for data processing.

3.2.1. Catalyst Preparation and Pretreatment

The following methods that are incipient-to-wetness impregnation of active metals and wash-coating of the cordierite monolithic support were applied to prepare catalysts that are used in this thesis.

3.2.1.1. Particulate Catalyst Preparation with Impregnation Method. La_2O_3 promoted MgO, La_2O_3 and SrO promoted MgO, La_2O_3 promoted CaO particulate catalysts each containing 10wt.%La_2O_3 and/or 10wt%SrO supported on MgO and/ or CaO were prepared by incipient to wetness impregnation technique of magnesium oxide support using the system in Figure 3.1 with an aqueous solution of $LaN_3O_9.6H_2O$ and aqueous solutions of $Sr(NO_3)_2$. Figure 3.1 shows the system which consists of a Retsch UR1 ultrasonic mixer, a vacuum pump, a Büchner flask and a MasterFlex computerized-drive peristaltic pump.

For the preparation of catalysts by incipient to wetness method, magnesium oxide support was first sieved into 30 mesh size and not calcined. Five grams of support was placed in a vacuum flask and was mixed under vacuum with an ultrasonic mixer for 30 minutes before impregnation.

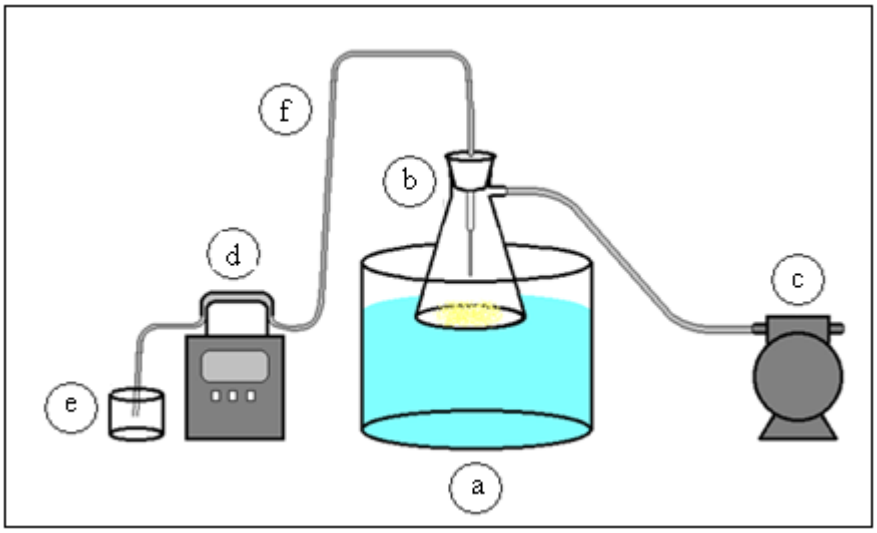

Figure 3.1. Schematic Diagram of the Impregnation System
(a) Ultrasonic Mixer, (b) Büchner Flask, (c) Vacuum Pump, (d) Peristaltic Pump, (e) Reactant Storage Tank and (f) Silicone Tubing.

All the metal salts were dissolved in 0.6 ml of deionized water per gram of magnesia support. Aqueous precursor solution was fed to the vacuum flask at a flow rate of 0.5 ml/min via silicone tubing. The slurry was mixed under vacuum by an ultrasound mixer to maintain uniformity of impregnation. Impregnated support was mixed for an additional 90 min.

To obtain La_2O_3 promoted MgO catalyst using lanthanum nitrate as precursor, the slurry obtained was dried in oven at 105 °C for 2 h, and then calcined in a muffle furnace at 850 °C for 4 h. (Gao *et al.,* 2010).

To prepare La_2O_3 and SrO promoted MgO, strontium nitrate as precursor of SrO and lanthanum nitrate as precursor of La_2O_3 are used. All the metal salts were dissolved in the required proportion in deionized water just sufficient to wet the MgO support, impregnate and the thick paste formed was dried at 120 °C for 12 h. The dried mass was crushed to 22-30 mesh size particles and then calcined at 950 °C for 10 h (Choudhary *et al.,* 1998).

For the La-promoted CaO catalysts with La/Ca mole ratio of 0.05; the precursors for La_2O_3 and CaO were thoroughly mixed with grinding in presence of water just sufficient to form a thick paste, which was dried at 120 °C for 12 h. The dried precursor catalyst mass was pressed binder-free, crushed to 22-30 mesh size particles and then calcined at 950 °C in a muffle furnace for 10 h (Rane *at al.,* 2010).

3.2.1.2. Preparation and Pretreatment of Monolithic Support with Wash-coating. The commercial cordierite monolithic support (Kale Porselen, Mullite C530) in Figure 3.2, was cut into the dimensions of 17 mm length and 8 mm diameter so that it can be easily placed into the 10 mm ID quartz tube reactor.

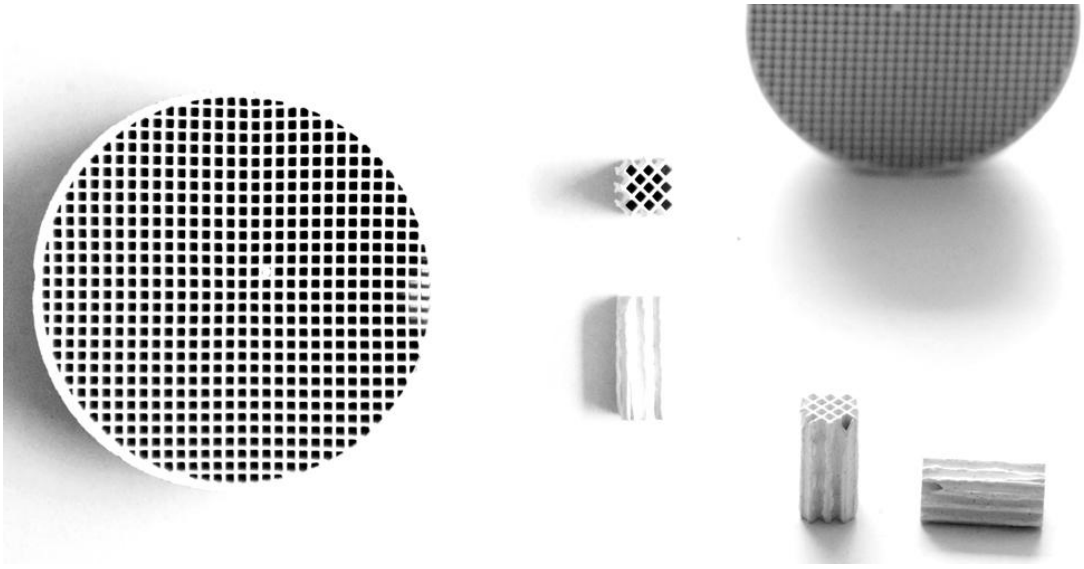

Figure 3.2. The Monolithic Structure Used in the Experiments.

The shaped monoliths were washed with acetone in order to remove residues possibly happened during the cutting procedure and open the pores and then dried in the oven.

The uncoated monoliths were weighed first and then it was immerged vertically into the magnesium solution that contains 60 mesh sizes of magnesium oxide and appropriate amount of deionized water mentioned at particulate catalyst preparation section. At this stage, an ultrasonic mixer is used to interpenetrate homogenously all around the monoliths during 30 min. In every 10 min, the excess solution inside the channels was removed by flushing thoroughly with pressurized air, then the monoliths were dried in microwave oven operated at 180 W for 40 min. and weighed again (Figure 3.3).

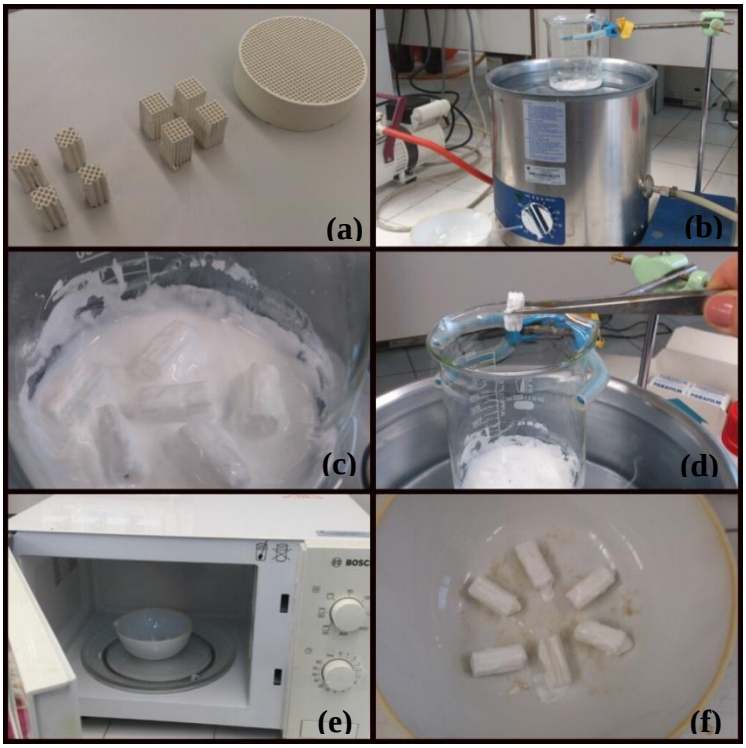

Figure 3.3. The Monolith Coating System (a) Shaping the Monolith to Suitable Size, (b) Preparing Aqueous Solution of Magnesium Oxide, (c) Dipping Procedure in Ultrasonic Mixer, (d) Compressed Air Flow, (e) Drying at Microwave Oven, (f) Coated Monoliths.

After the monolithic supports were coated with magnesium oxide, to get La_2O_3 promoted MgO catalyst, lanthanum nitrate is dissolved in sufficient amount of deionized water and coated monoliths were dipped over this aqueous solution of metal salts for 15 minutes. After every dipping process, the excess solution was evacuated from the monolith channels by a flow of compressed air and then dried in a microwave oven operated at 180 W for 40 min. This procedure was repeated until the monolith weight has minimally gained 35% of its tare weight. Finally, La_2O_3 promoted MgO monoliths were dried in oven at 105 °C for 2 h, and then calcined in a muffle furnace at 850 °C for 4 h.

To prepare La_2O_3 and SrO promoted MgO monoliths, which is prepared using strontium and lanthanum nitrate precursor, same procedure mentioned above is followed but at the final stage, the coated monoliths were dried at 120 °C for 12 h and then calcined at 950 °C for 10 h.

3.2.2. Catalytic Reaction System for OCM Reaction

1/4", 1/8" and 1/16" OD stainless steel and copper tubing, valves with stainless steel and brass fittings for feeding gaseous species were used in the system. The flow rates of research grade high purity gases (oxygen, helium) from pressurized cylinders passed through the system were regulated with Omega Model 5878 digital mass flow controllers of which set values were adjusted by the main control unit. Additionally, methane gas was delivered to the system with Brooks 5850E mass flow controllers.

Reactant gases (oxygen and methane) without diluents, after being mixed, were sent into the reaction section which consists of 10 and 20 mm ID and 80.5 cm long fixed bed down flow quartz reactor; 10 mm ID quartz becomes narrow to 2 mm ID quartz to minimize the void volume after catalyst bed. (Figure 3.4), The reactor was longer than the furnace tube so that the fittings of the reactor can be kept out of the furnace to facilitate manipulation during catalyst charging or recharging.

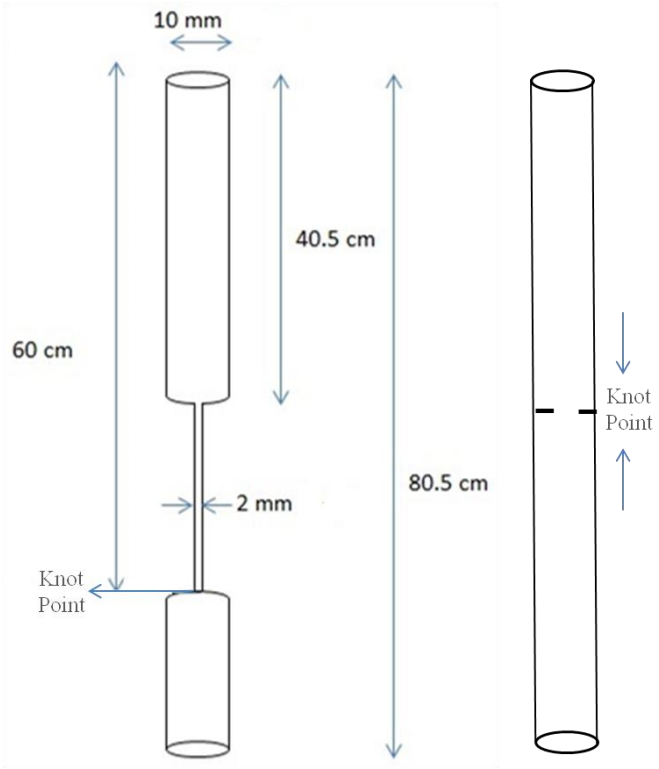

Figure 3.4. 10 mm (left) and 10 to 2 mm Narrower (right) ID Quartz Fixed-Bed Down Flow Reactor Scheme.

Quartz tubes were connected with two custom design fittings to the 1/4" stainless steel main line. The quartz reactor placed in a 30 mm ID 600 mm long furnace having 10 cm long constant temperature zone controlled to ±0.1 K by a Shimaden FP-21 programmable temperature controller. The furnace that heats the reactor was heated up with 10 $^{\circ}$C/min. In the reactant entering and product leaving from the reactor part, there is two ON-OFF valves to either the GC sampling or to outside passing through the soap bubble meter for measuring the flow rate.

The catalyst bed used in this work for the particulate catalyst and wash-coated monolith catalyst are given in Figure 3.5. The tests were done at various temperatures between 620 °C and 700 °C, with total feed stream was 100 ml/min in atmospheric pressure with different CH_4/O_2 molar ratio.

Particulate catalysts were inserted into the 10 mm ID quartz down flow reactor. The quartz tube reactor was modified narrowing to 2 mm in the middle to remove the gasses quickly after the catalyst layer. Both side of the reactor filled with quartz chips, silica particles or quartz sand as seen at Figure 3.5.

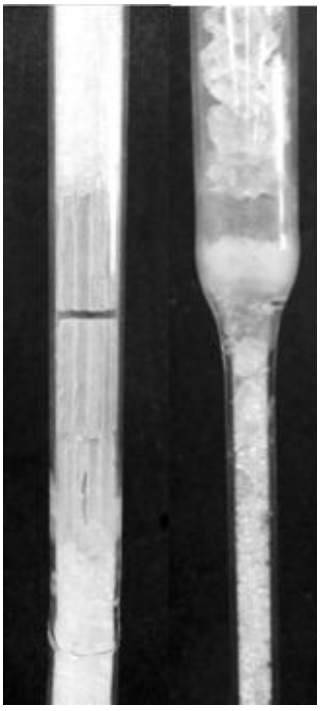

Figure 3.5. (a) Monoliths, (b) Particulate Catalyst.

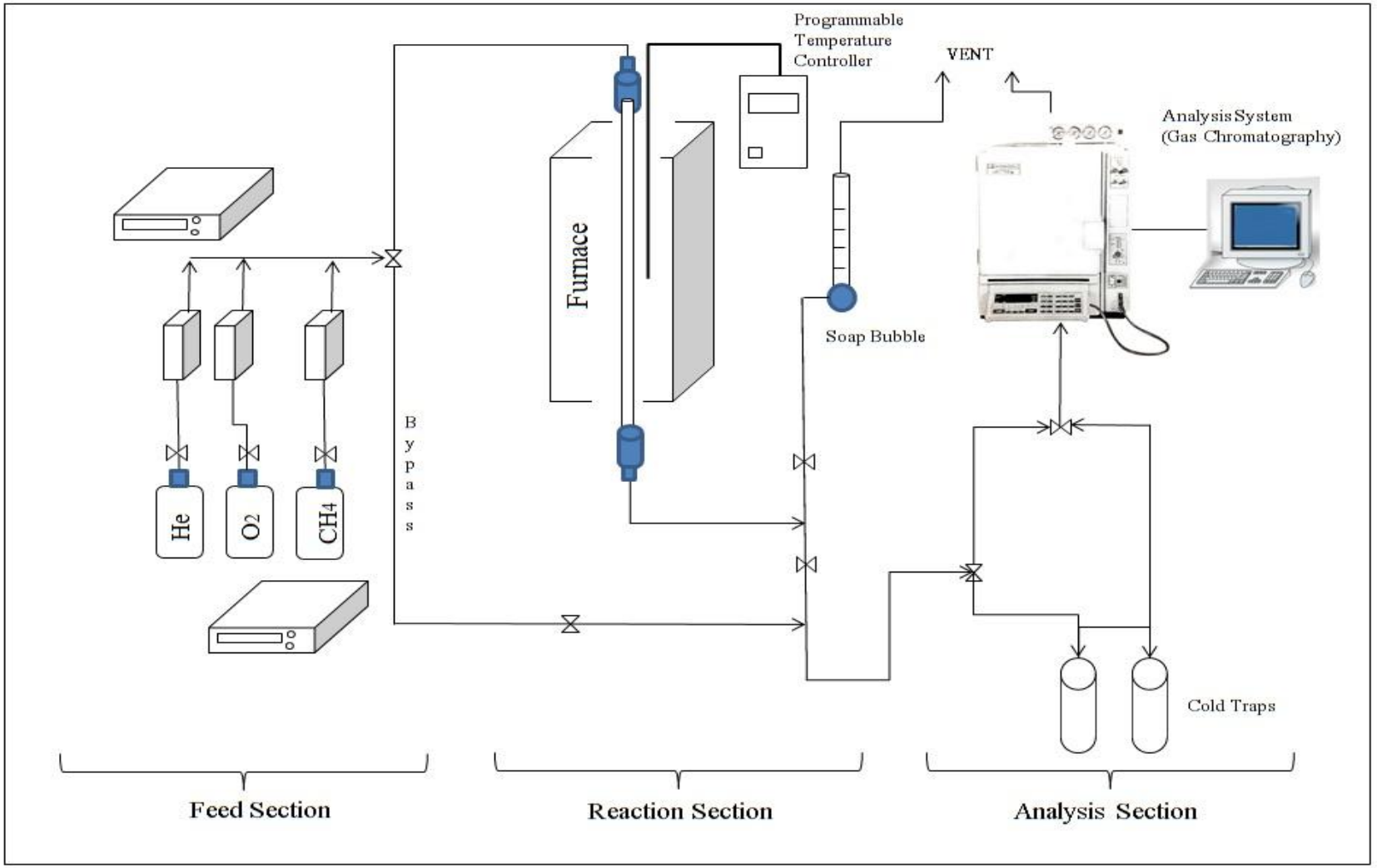

Figure 3.6. The Micro Reactor Flow System and Product Analysis System (Düşova, 2014).

Coated monoliths were filled in the 10 mm ID quartz tube reactor. In each experiment, three coated cordierite monoliths were used (Figure 3.5). One bare monolith catalyst support weight is around 0.810 gr., when its coated approximate weight is 1.210 gr. (It's catalyst weight was around 0.350 gr.); hence three monoliths had catalyst approximately equal to the amount of particulate catalyst used. After monoliths placed at the reactor, both of the bottom and top side were filled with quartz chips, silica particles or quartz sand.

3.2.3. Product Analysis System for OCM reaction

During the experiments, the product mixture contained unreacted methane, oxygen and product gases involving hydrogen, carbon monoxide, carbon dioxide, ethylene and ethane. The water vapor produced as a result of the reaction was removed via cold trap at the end of the reactor to prevent possible damages at the GC. A Shimadzu GC–14A (Figure 3.7) gas chromatograph equipped with a Thermal Conductivity Detector (TCD) was used to analyse feed and product streams. Analysis conditions were given in Table 3.3.

Figure 3.7. Gas Chromotography Instrument Used in the Experiments (Shimadzu GC-14A).

Table 3.3. Reactant and product gas analysis conditions.

GC	A Shimadzu GC – 14A
Detector Type	TCD
Column Temperature, °C	200
Injector Temperature, °C	170
Detector Temperature, °C	230
Detector Current, mA	100
Carrier Gas	Helium
Carrier Gas Flow rate, ml/min	25
Column Packing Material	Carboxen 1000, 80-60 mesh
Column Tubing Material	Cupper
Column Length & ID	210 x 3 mm
Sample Loop	1 mL

4. RESULTS AND DISCUSSIONS

In this work, the experiments are conducted using both particulate wash-coated monolith catalysts using the best catalyst formulations and experimental conditions reported in the literature. The effects of following parameters on the reaction yield were investigated and reported through this section:

- Catalyst content.
- Catalyst form (particulate or wash-coated monolith)
- Reaction temperature and CH_4/O_2 ratio
- Filling material used in empty space in reactor
- Reactor ID
- Diluent gas

4.1. Performance Tests

The catalytic activity tests under various reaction conditions were performed, and the results were reported as CH_4 conversion (x_{CH_4}), C_2 selectivity (S_{C_2}) and C_2 yield (Y_{C_2}), which were calculated by using the following formulas:

$$x_{CH_4} = CH_4 \text{ conversion}(\%) = \left[\frac{[CH_4]_{in} - [CH_4]_{out}}{[CH_4]_{in} - [CH_4]_{out} \times \frac{5}{8}}\right] \times 100 \quad (4.1)$$

$$S_{C_2}(\%) = \left[\frac{2 \times ([C_2H_4]_{product} + [C_2H_6]_{product})}{[2 \times ([C_2H_4]_{product} + [C_2H_6]_{product})] + [CO]_{out} + [CO_2]_{out}}\right] \times 100 \quad (4.2)$$

$$Y_{C_2} = C_2 \text{ yield } (\%) = \left[x_{CH_4} \times S_{C_2}\right]/100 \quad (4.3)$$

The best results obtained were summarized in Table 4.1 with the experimental conditions studied and the detailed results were presented and discussed in the remaining sections. The experimental error was within the 15% through the study.

Table 4.1. Experimental results of particulate and monolith catalysts.

Exp #	(P)/ (M)	Catalyst Type	Temp (°C)*	Feed (ml/min)	CH_4/O_2	He (ml/min)	χ_{CH_4} (%)	S_{C_2} (%)	Y_{C_2} (%)
1	P	10%La_2O_3/MgO	800	70	4/1	20	47.2	5.2	2.5
2	M	10%La_2O_3/MgO	750	70	4/1	20	39.8	17.6	7
3	M	10%La_2O_3/MgO	750	70	4/1	-	40.1	17.8	7.1
4	P	10%La_2O_3/MgO	650	70	7/1	-	39.8	10.7	4.2
5	P	10%SrO/ 10%La_2O_3/MgO	650	100	7/1	20	36.2	22.1	8
6	M	10%SrO/10% La_2O_3/MgO	650	100	7/1	20	45.8	24.7	11.3
7	P	10%La_2O_3/CaO	650	120	7/1	-	24.5	15.8	3.8
8	P	10%SrO/MgO	660	120	7/1	-	28.5	23.2	6.6
9	M	10%SrO/MgO	660	120	11/1	-	35.7	27.1	9.7
10	P	10%La_2O_3/MgO	680	128	15/1	-	38.1	15.4	5.8
11	M	10%La_2O_3/MgO	680	128	15/1	-	44.8	17.1	7.7
12	M	10%SrO/10% La_2O_3/MgO	650	128	15/1	-	32.2	45	14.5
13	M	10%SrO/10% La_2O_3/MgO	650	128	11/1	-	29.3	42.8	12.5
14	M	20%SrO/10% La_2O_3/MgO	650	128	15/1	-	29.8	34.7	9.3
15	M	10%SrO/20% La_2O_3/MgO	650	128	15/1	-	25.6	39.8	10.1
16	M	La_2O_3	680	128	15/1	-	30.2	15.8	4.7
17	M	SrO	680	128	15/1	-	24.2	9.1	2.2
18	P	10%SrO/10% La_2O_3/MgO	650	128	15/1	-	32.3	29.8	9.6
19	P	10%SrO/10% La_2O_3/MgO (#18 treated O_2)	650	128	15/1	-	28.8	24.8	7.1
20	P	10%SrO/10% La_2O_3/MgO (#19 treated O_2)	650	128	15/1	-	23.9	20.7	4.9
21	P	10%SrO/ 10% La_2O_3/ MgO (#20 treated O_2)	650	128	15/1	-	24.6	17.4	4.2

***** Experiments are conducted in the temperature range of 620-700 °C, where the maximum yield has been observed.

4.1.1. Effect of Content and Form of Catalyst

10wt.%La_2O_3/MgO, 10wt.%SrO/MgO, 10wt.%La_2O_3/10wt.%SrO/MgO and 10wt.%La_2O_3/CaO particulate catalysts (Table 4.2) were tested first at the temperature of 650°C and CH_4/O_2 of 7 (Figure 4.1). The highest yield (8%) was achieved in 10wt.%La_2O_3/10wt.%SrO/MgO with 36.2% conversion and 22.1% selectivity.

Choudhary *et al.* (1998) reached 20.5% CH_4 conversion and 14% C_2 selectivity in the experiments conducted at CH_4/O_2 of 8 and temperature of 800°C using the same catalyst. Yu *et al.* (1997) discussed the effect of La_2O_3 and SrO on reaction. They argued that the lanthanum oxide might be an inhibitor of methyl radical or methane oxidation into CO while strontium oxide might play the role of an inhibitor of the gas-phase oxidation of ethylene.

Table 4.2. Comparison of different type particulate catalyst.

(P)/(M)	Catalyst Type	Temp. (°C)	Feed (ml/min)	CH_4/O_2	He (ml/min)
P	10%La_2O_3/CaO	650	120	7/1	-
P	10%La_2O_3/MgO	650	70	7/1	-
P	10%SrO/10%La_2O_3/MgO	650	100	7/1	20

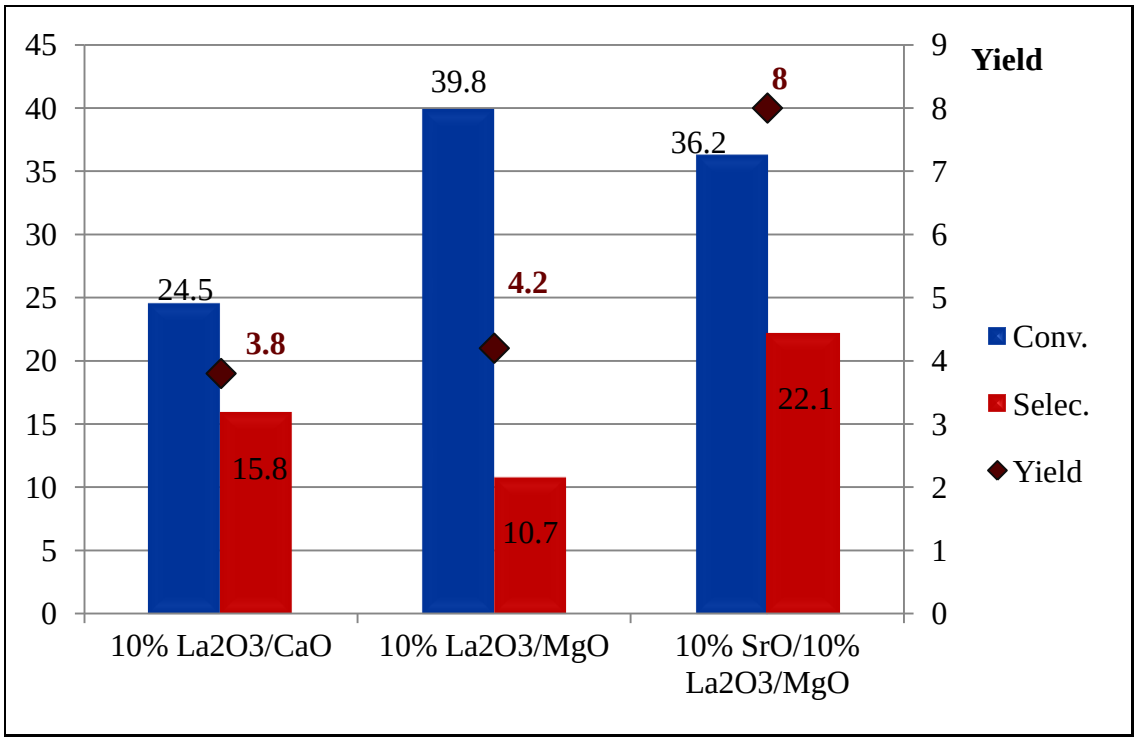

Figure 4.1. Comparison of the Different Type Particulate Catalyst at $CH_4/O_2 = 7$ and Temperature at 650 °C.

Next, various catalysts contents were tested and compared in the wash-coated monolith form as presented in Table 4.3 and Figure 4.2. However, this time only MgO support was used (considering that CaO support did not performed as well as MgO in particulate form), and 100% SrO and 100% La_2O_3 were also tested. Again 10wt.% La_2O_3/SrO/MgO gave the highest yield. Although much higher CH_4 conversion was achieved over 10wt.% La_2O_3/MgO, the C_2 selectivity was the highest over 10wt.% La_2O_3/SrO/MgO resulting a better yield.

It should be also noted that the yield obtained over wash-coated monolith (14.5%) was much higher that that obtained over particulate catalyst (8%). The same was true for 10wt.% La_2O_3/MgO; the monolithic form had much better yield (7.7%) than the particulate catalyst (4.2%). Apparently the presence of empty space in the monolith channels improves the yield as it was suggested by Arndt *et al.* (2011).

Table 4.3. Comparison of different type monolith catalyst.

(P)/(M)	Catalyst Type	Temp.(°C)	Feed (ml/min)	CH_4/O_2
M	SrO	680	128	15/1
M	La_2O_3	680	128	15/1
M	10%La_2O_3/MgO	680	128	15/1
M	10%SrO/MgO	680	120	11/1
M	10%SrO/10%La_2O_3/MgO	680	128	15/1

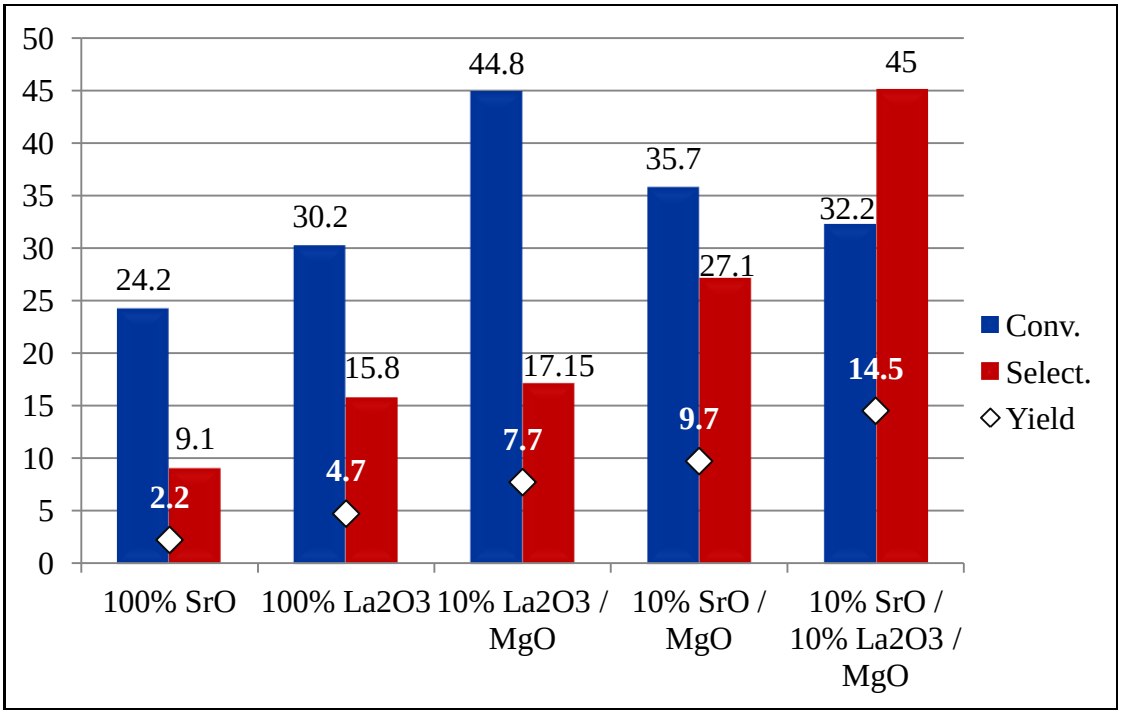

Figure 4.2. Comparison of the Different Type Catalyst on Monolith at CH_4/O_2 = 7 and temperature at 680 °C.

4.1.2. Effect of CH_4/O_2 Ratio in Feed Stream

To observe the effect of the CH_4/O_2 molar flow rate in the feed stream, both 10wt.% La_2O_3/MgO and 10wt.%La_2O_3/10wt.%SrO/MgO catalysts were tested under various CH_4/O_2 ratios over both particulate and monolith form. Figure 4.3 shows the effect of

CH_4/O_2 molar flow rate on particulate 10wt.%La_2O_3/MgO catalyst. The conversion decreased by increasing of the CH_4/O_2 molar flow rate ratio from 4 to 15 but the selectivity and yield increased reaching the highest value of yield at 5.8 % at the CH_4/O_2 ratio of molar flow rate is 15. The behavior of monolithic 10wt.% La_2O_3/MgO was quite different; increasing the CH_4/O_2 molar flow rate from 4 to 15, increased both conversion and yield increase while the selectivity did not change significantly (Figure 4.4). Apparently monolithic form provides better dispersion and probably more contact time allowing higher conversion considering that the catalyst bed length is higher in monolithic form.

It is surprising that the results for the 10wt.% La_2O_3/10wt.% SrO/MgO was also quite different. The CH_4 conversion was not changed significantly when CH_4/O_2 ratio increased from 7 to 15 but the selectivity increased significantly from 10.7 to 15.4% over the particulate catalyst (Figure 4.5). The results over monolithic form were also similar for selectivity. The conversion of CH_4, however, was also unchanged by changing CH_4/O_2 ratio from 7 to 15 but decreased from 3 to 7 (Figure 4.6).

Borchert *et al.* (1997) demonstrated that the strontium promoter effect on La_2O_3 was associated with increase of lattice oxygen mobility due to anionic vacancies created in the solid when Sr^{2+} replaces La^{3+}. Therefore, strontium reduces catalyst sintering, favoring the hexagonal 0 0 1 crystalline orientation at higher calcination temperatures (950 °C), maintaining high C_2 selectivity.

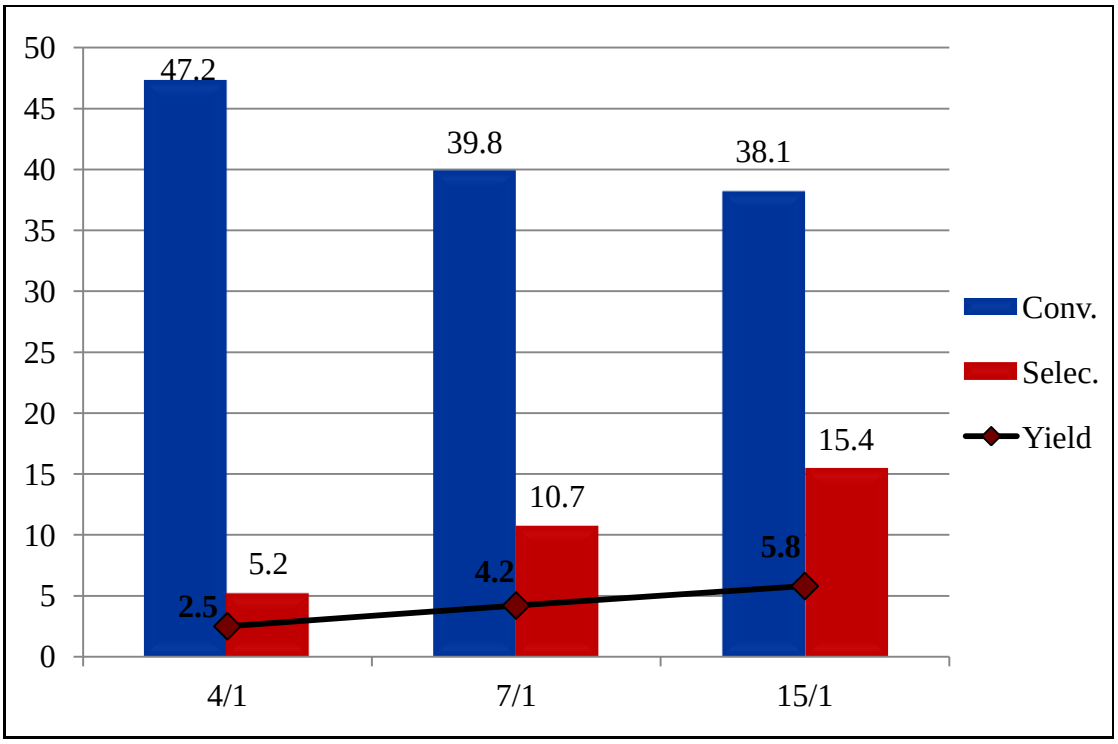

Figure 4.3. The Effect of CH_4/O_2 Molar Flow Rate on Particulate 10wt.% La_2O_3/MgO Catalyst (Reaction Temperature is 650 °C).

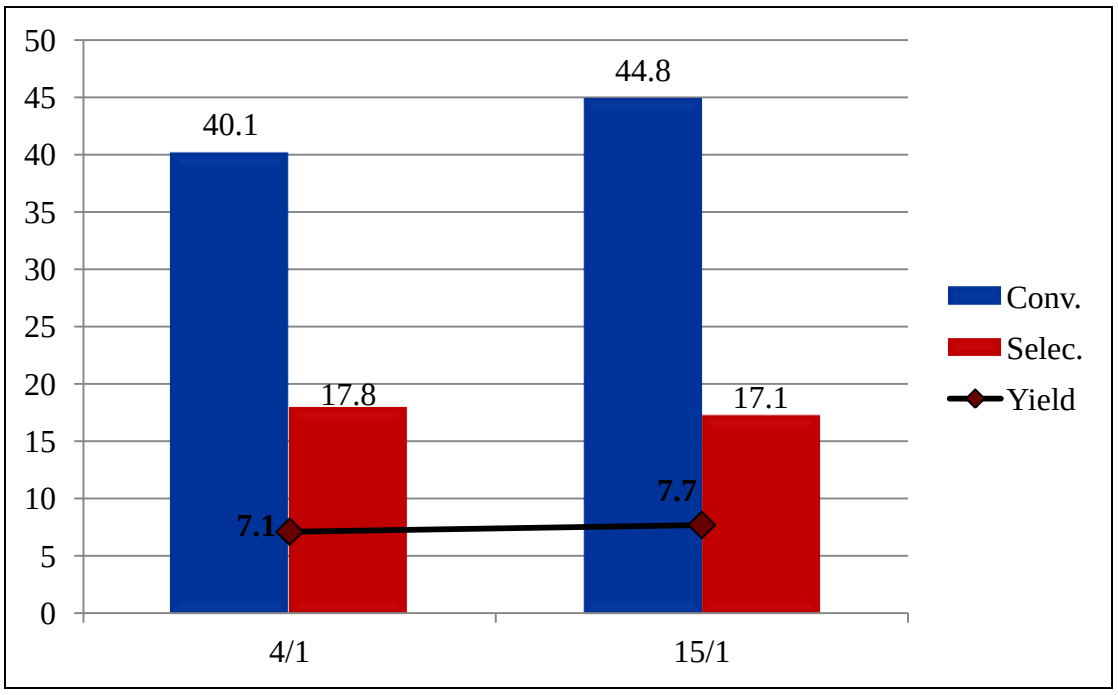

Figure 4.4. The Effect of CH_4/O_2 Molar Flow Rate on Monolith 10wt.% La_2O_3/MgO (Reaction Temperature is 680 °C).

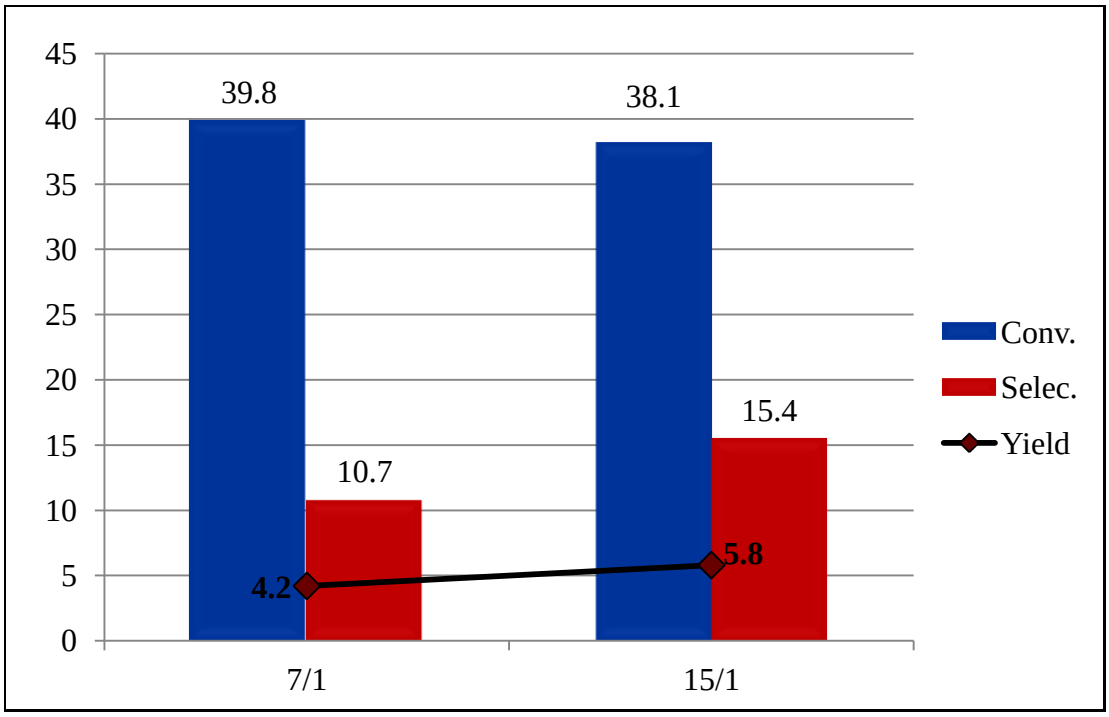

Figure 4.5. The Effect of CH_4/O_2 Molar Flow Rate on Particulate 10wt.% La_2O_3/10wt.% SrO/MgO (Reaction Temperature is 650 °C).

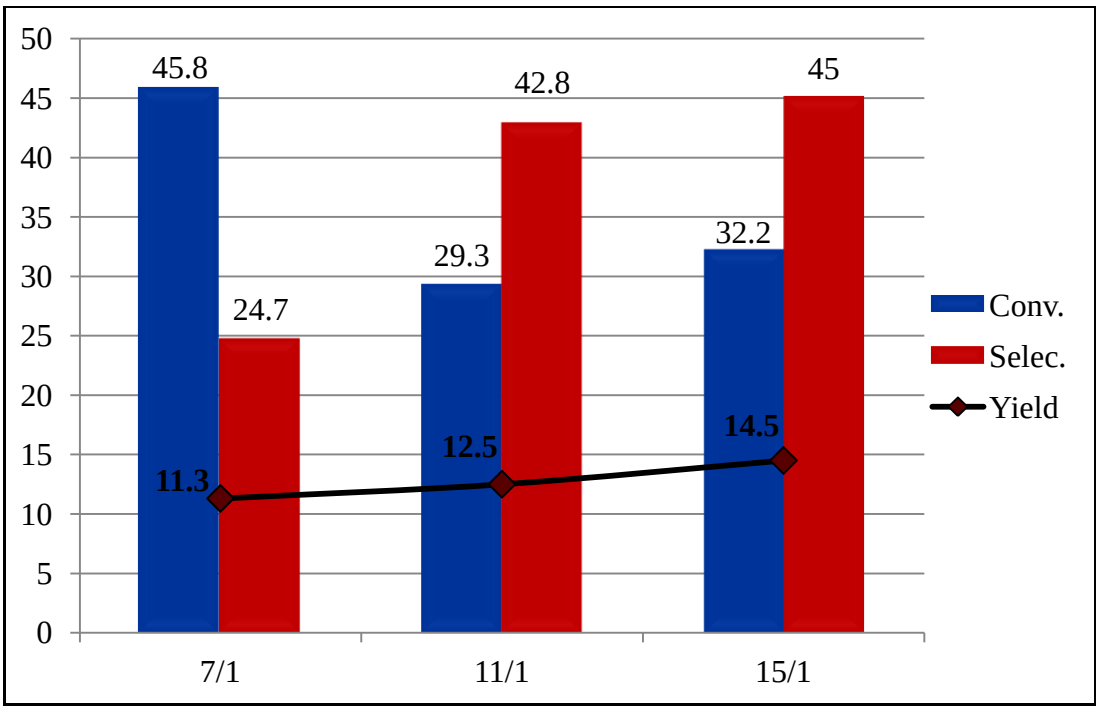

Figure 4.6. The Effect of CH_4/O_2 Molar Flow Rate on Monolith 10wt.%La_2O_3/10wt.% SrO/MgO (Reaction Temperature is 650 °C).

4.1.3. Effects of Metal Loadings to Cordierite Monolith

To investigate the effect of the metal loading over monolith catalysts, three catalysts having different La_2O_3/SrO percentages (10/20, 10/10 and 20/10) were compared at the reaction temperature of 650 °C and CH_4/O_2 ratio of 15/1 (Figure 4.7). All three catalysts gave higher C_2 yields than the catalyst containing only one of these metal oxides; however, the highest CH_4 conversion and C_2 selectivity (therefore highest yield) was obtained over 10wt.%La_2O_3/10wt.%SrO/MgO catalysts. Even though the synergic effects of two metal oxides seem to enhance the performance in all three cases, the excess use of any of these negatively affects this enhancement.

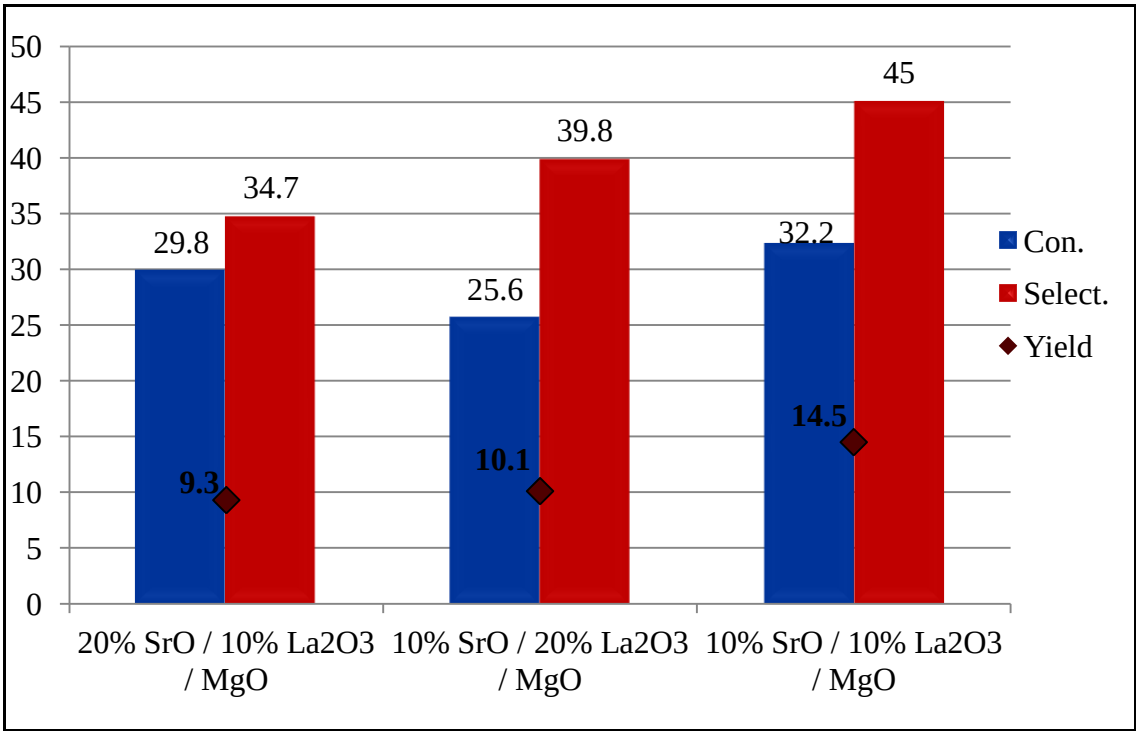

Figure 4.7. Effect of the Different Ratio of the Metal Loading on Monolith (Temperature 650 °C and CH_4/O_2 is 15/1).

4.1.4. Effect of the Temperature

Effect of temperature, from 620 °C to 680 °C, on the performance was investigated over various catalyst formulation and form at the CH_4/O_2 ratio of 15. It should be noted that the temperature reported as the reaction temperatures are the values measured outside the quartz reactor. The actual temperature is expected to be up to 150 °C as measured in various similar studies (Lunsford, 2000). Figure 4.8-4.16 show behaviors of the catalysts discussed in previous sections. Although the behavior of different catalysts against the temperature change are also different in details, the yield is usually exhibits a maximum around 650-650 °C. In all cases, the selectivity increases first and then decreases with further increase in temperature as expected since higher temperatures also increases product decomposition. The conversion is also exhibits similar behaviors probably due to O_2 depletion (all oxygen was consumed after a certain temperature depending on the catalyst and CH_4/O_2 ratio).

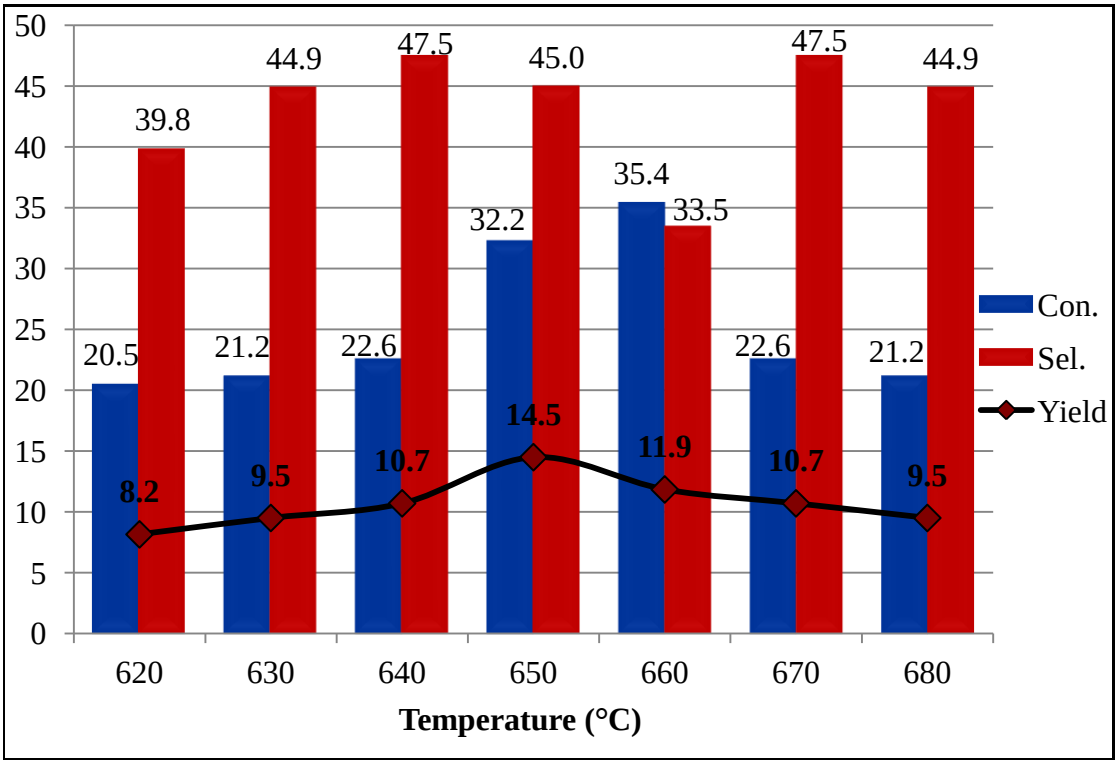

Figure 4.8. Effect of Temperature on Conversion, Selectivity and Yield for 10wt.% La_2O_3/10wt.% SrO/MgO Monolith (CH_4/O_2: 15/1).

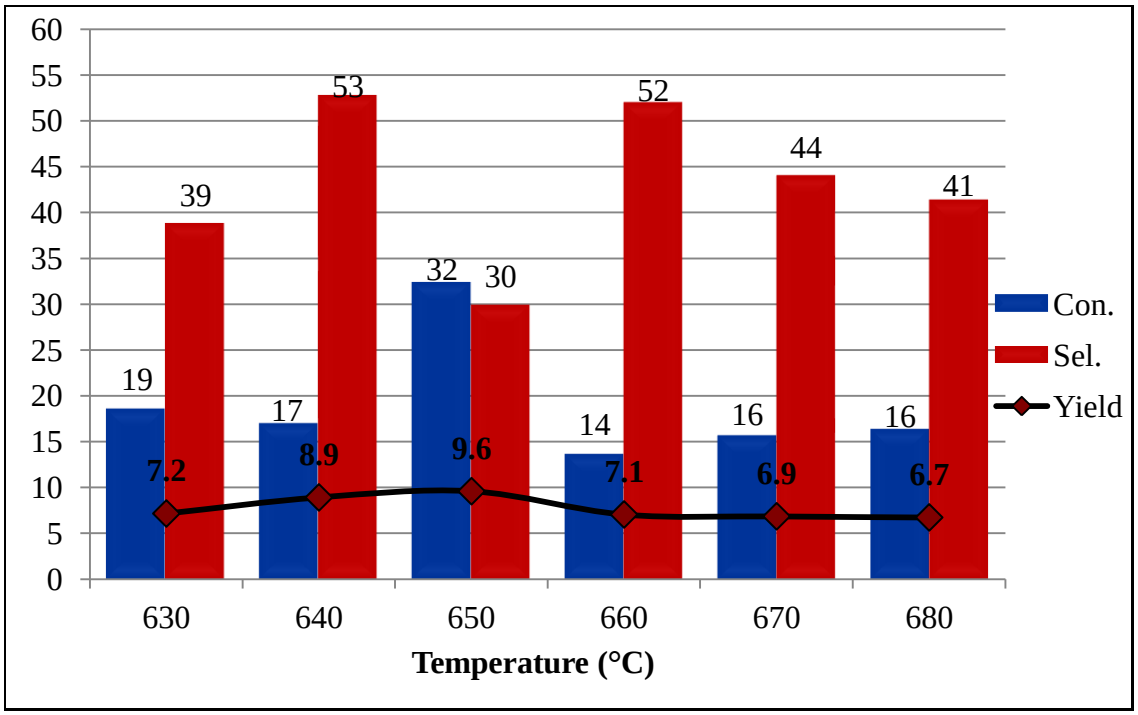

Figure 4.9. Effect of Temperature on Conversion, Selectivity and Yield for 10wt.% La_2O_3/10wt.% SrO/MgO Particulate Catalyst (CH_4/O_2: 15/1).

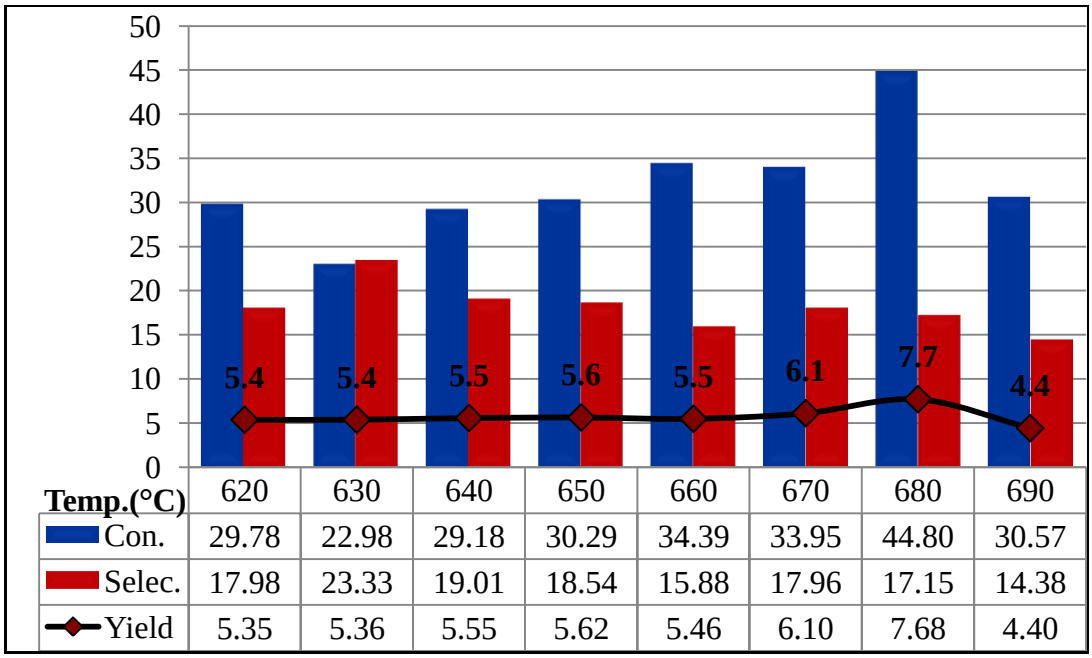

Temp.(°C)	620	630	640	650	660	670	680	690
Con.	29.78	22.98	29.18	30.29	34.39	33.95	44.80	30.57
Selec.	17.98	23.33	19.01	18.54	15.88	17.96	17.15	14.38
Yield	5.35	5.36	5.55	5.62	5.46	6.10	7.68	4.40

Figure 4.10. Effect of Temperature on Conversion, Selectivity and Yield for 10wt.% La_2O_3 /MgO Monolith (CH_4/O_2: 15/1).

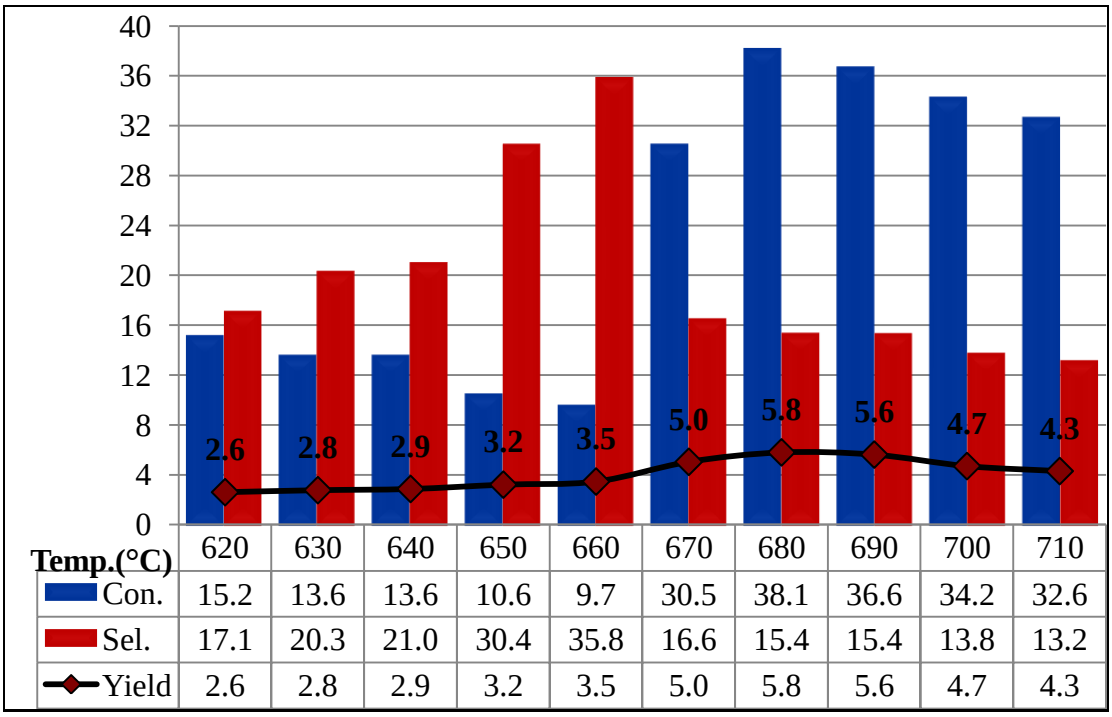

Temp.(°C)	620	630	640	650	660	670	680	690	700	710
Con.	15.2	13.6	13.6	10.6	9.7	30.5	38.1	36.6	34.2	32.6
Sel.	17.1	20.3	21.0	30.4	35.8	16.6	15.4	15.4	13.8	13.2
Yield	2.6	2.8	2.9	3.2	3.5	5.0	5.8	5.6	4.7	4.3

Figure 4.11. Effect of Temperature on Conversion, Selectivity and Yield for 10wt.% La_2O_3 /MgO Particulate Catalyst (CH_4/O_2: 15/1).

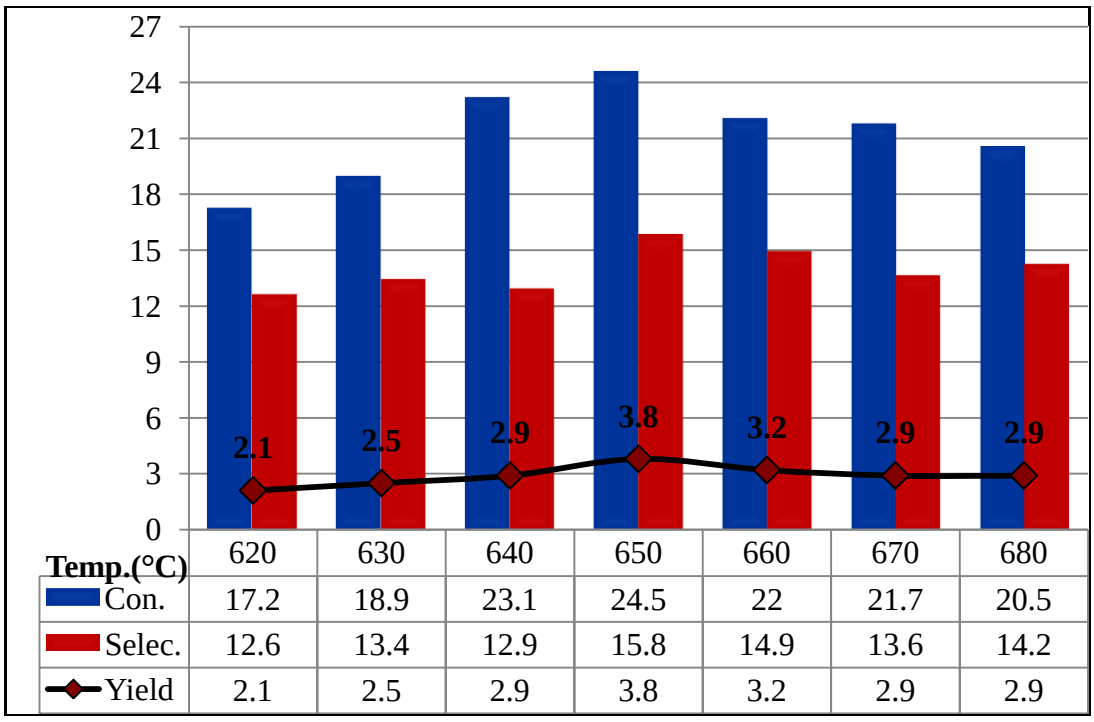

Temp.(°C)	620	630	640	650	660	670	680
Con.	17.2	18.9	23.1	24.5	22	21.7	20.5
Selec.	12.6	13.4	12.9	15.8	14.9	13.6	14.2
Yield	2.1	2.5	2.9	3.8	3.2	2.9	2.9

Figure 4.12. Effect of Temperature on Conversion, Selectivity and Yield for 10% La_2O_3/CaO Particulate Catalyst (CH_4/O_2: 15/1).

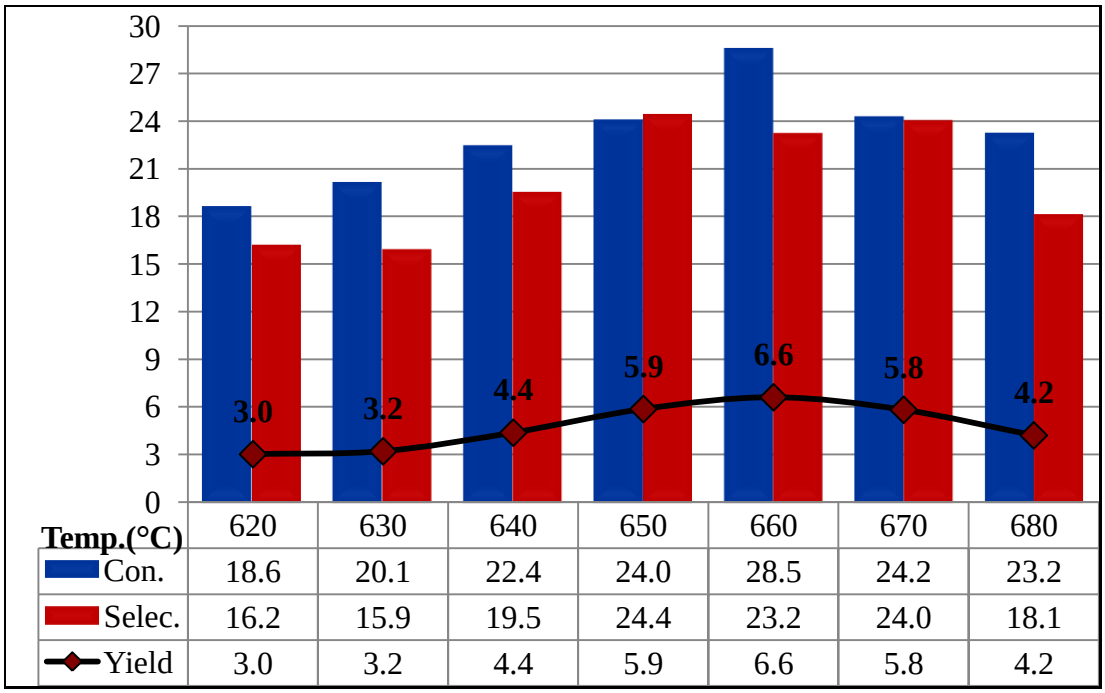

Temp.(°C)	620	630	640	650	660	670	680
Con.	18.6	20.1	22.4	24.0	28.5	24.2	23.2
Selec.	16.2	15.9	19.5	24.4	23.2	24.0	18.1
Yield	3.0	3.2	4.4	5.9	6.6	5.8	4.2

Figure 4.13. Effect of Temperature on Conversion, Selectivity and Yield for 10wt.% SrO/MgO Particulate Catalyst (CH_4/O_2: 15/1).

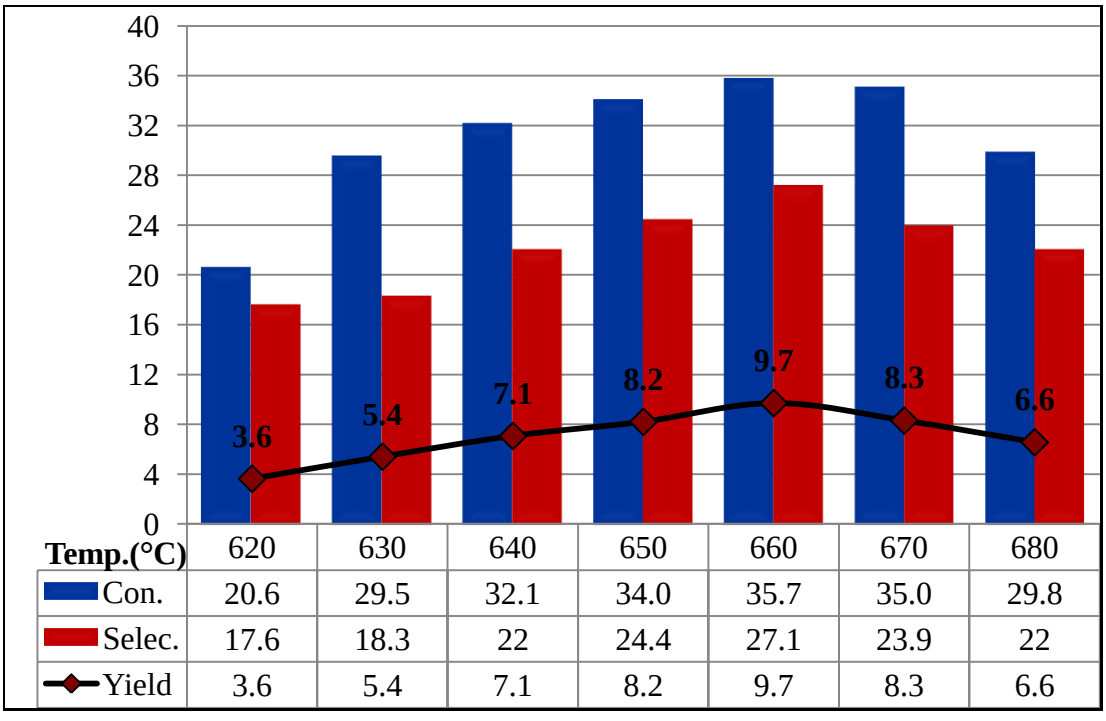

Temp.(°C)	620	630	640	650	660	670	680
Con.	20.6	29.5	32.1	34.0	35.7	35.0	29.8
Selec.	17.6	18.3	22	24.4	27.1	23.9	22
Yield	3.6	5.4	7.1	8.2	9.7	8.3	6.6

Figure 4.14. Effect of Temperature on Conversion, Selectivity and Yield for 10% SrO/MgO Monolith (CH_4/O_2: 15/1).

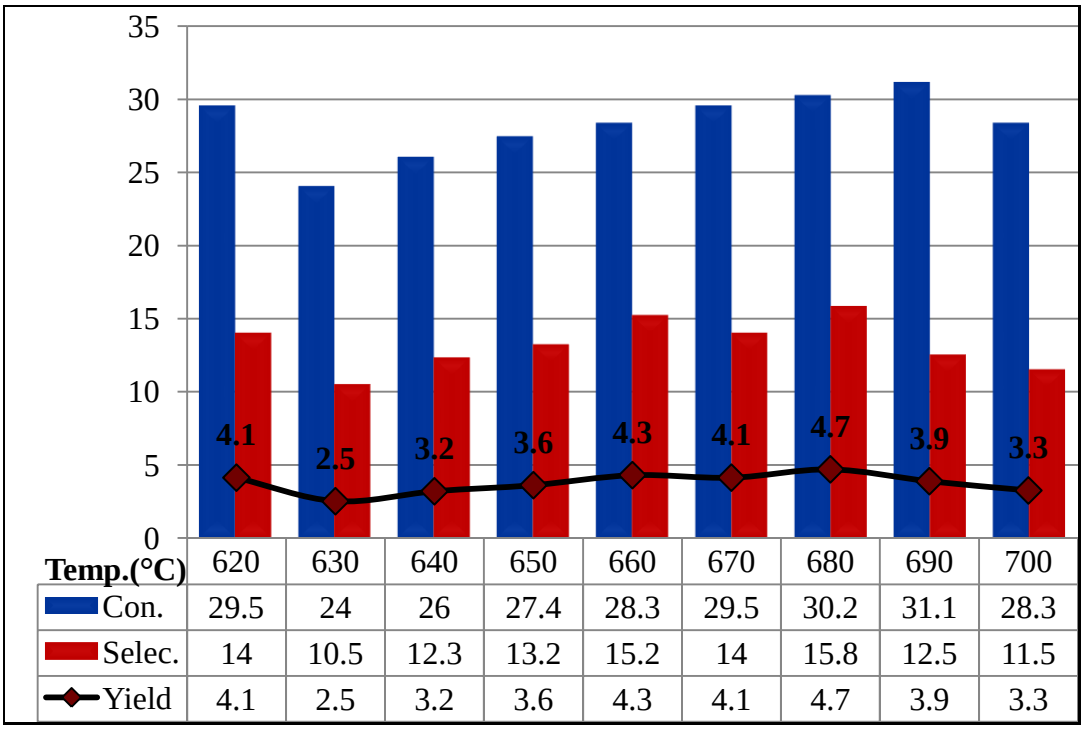

Temp.(°C)	620	630	640	650	660	670	680	690	700
Con.	29.5	24	26	27.4	28.3	29.5	30.2	31.1	28.3
Selec.	14	10.5	12.3	13.2	15.2	14	15.8	12.5	11.5
Yield	4.1	2.5	3.2	3.6	4.3	4.1	4.7	3.9	3.3

Figure 4.15. Effect of Temperature on Conversion, Selectivity and Yield for 100%SrO Monolith (CH_4/O_2: 15/1).

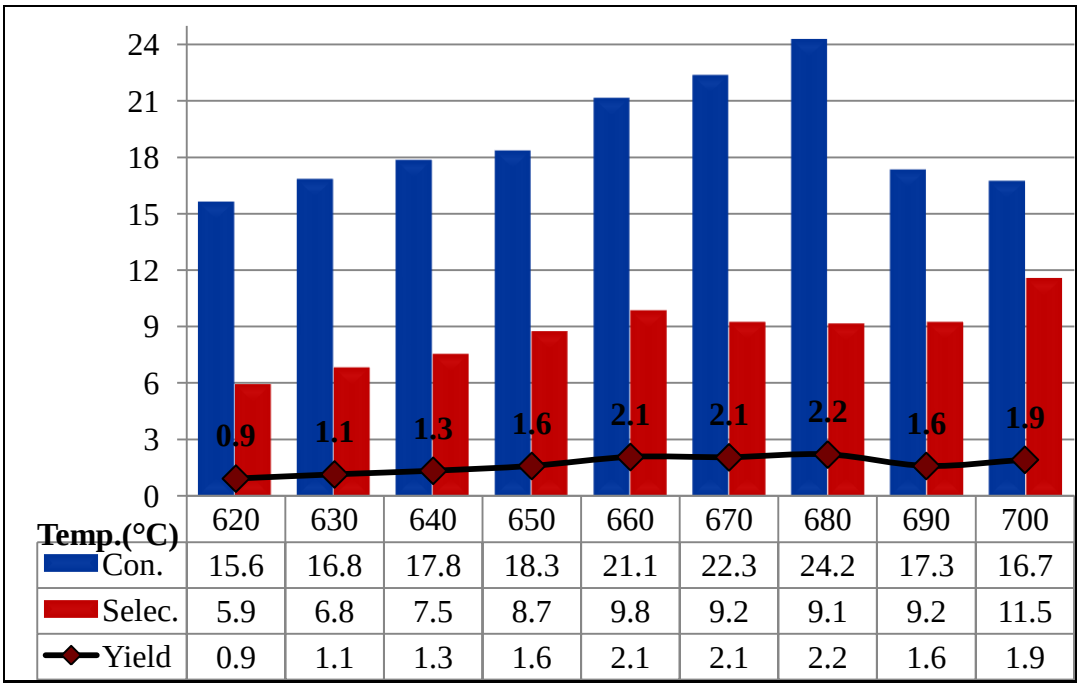

Temp.(°C)	620	630	640	650	660	670	680	690	700
Con.	15.6	16.8	17.8	18.3	21.1	22.3	24.2	17.3	16.7
Selec.	5.9	6.8	7.5	8.7	9.8	9.2	9.1	9.2	11.5
Yield	0.9	1.1	1.3	1.6	2.1	2.1	2.2	1.6	1.9

Figure 4.16. Effect of Temperature on Conversion, Selectivity and Yield for 100% La_2O_3 Monolith (CH_4/O_2: 15/1).

4.1.5. Effect of Reactor Diameter

At the beginning of the experiments, 10mm ID quartz tube reactor was used to place cordierite monolithic support. To avoid gas phase reactions, a new quartz tube reactor was designed with the diameter of 10 mm is narrowing down to 2 mm as shown in the Figure 3.5. As a result of this design change, both CH_4 conversion and the C_2 selectivity were increased when the experiment was done with particulate catalyst (Figure 4.18), and the remaining experiments were conducted with this design. This result is similar to those observed by other investigators like Lunsford (1998) was used fused-quartz tubing reactor with the internal diameter decreasing from 7mm to 2 mm objective to increase the residence time after the catalyst to avoid decomposition of products in gas phase reactions.

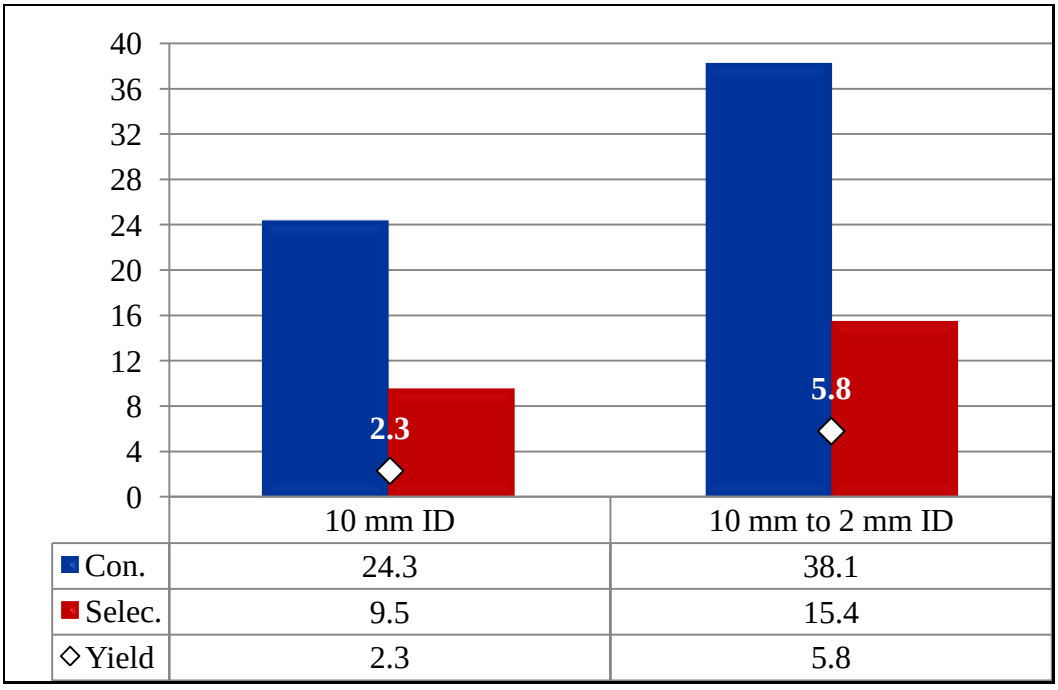

	10 mm ID	10 mm to 2 mm ID
Con.	24.3	38.1
Selec.	9.5	15.4
◇Yield	2.3	5.8

Figure 4.17. Investigation for the Reactor Tube Diameter to Reaction Performance Using 10wt.%La_2O_3/MgO Particulate Catalyst
(Reaction Temperature at 680 °C, CH_4/O_2 Ratio is 15).

4.1.6. Effect of Reactor Filling Material

According the researchers like Choudhary (1998) and Ji *et al.* (2003), C_2 selectivity can be increased by filling the space above and below the catalyst bed with some porous material to decrease the temperature gradient in the catalyst, bed and minimize the contribution of gas phase reactions that decompose products. Düşova (2014) conducted some experiments with porous material like pure crushed SiO_2, quartz sand, 18-140 mesh size quartz chips, uncrushed-3/16 inches spheres of α-Al_2O_3 particles and larger sizes quartz chips. According to her findings, filling with the large size quartz chips showed the best catalytic activity and doubled the C_2 selectivity at around approximately the same CH_4 conversion level. In this work, the large size quartz chips and quartz wool was tested as filling materials, and no difference was observed between them. Therefore, the quartz chips were used in the rest of experiments.

4.1.7. Effect of Diluent Gas in the Feed Stream

To understand effect of feed dilution, the feed containing 80% CH_4, 20%O_2 was compared 60% CH_4, 15% O_2 and 25% He; both feed had the CH_4/O_2 ratio of 4. As can be seen from Figure 4.18, the yield remained almost get. After this conclusion, the diluent gas was not added to feed stream in the remaining experiments.

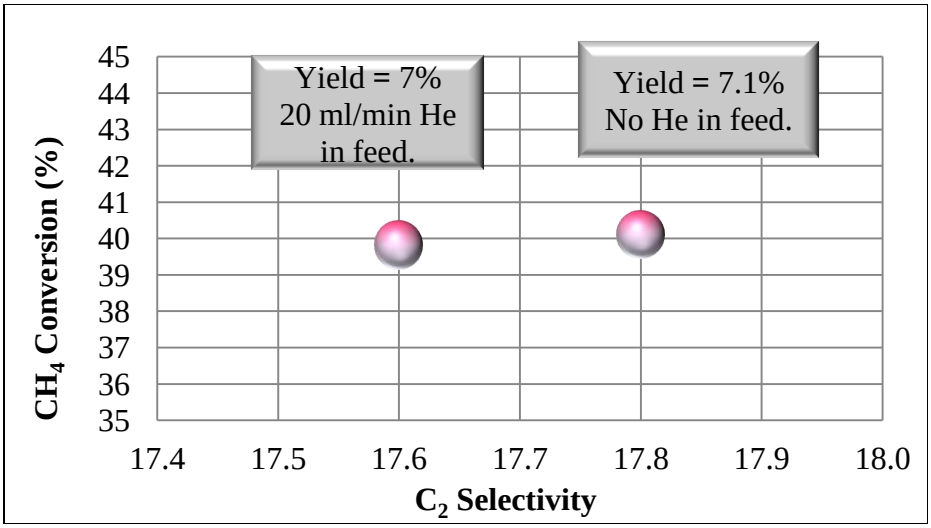

Figure 4.18. The effect of the Diluent Gas on Reaction Performance Using 10wt.% La_2O_3/MgO Particulate Catalyst (Reaction Temperature at 750 $^{\circ}$C, CH_4/O_2 ratio is 4).

4.1.8. Regeneration of Monolithic Catalyst by Oxygen Treatment

The stability of best performing catalyst (10wt.%La_2O_3/10wt.%SrO/MgO in monolithic form) was also tested at 650 °C when CH_4/O_2 ratio was 15. To do this, the 20% oxygen in He carrier passed through the used catalyst for about one hour at 800 °C, and used again. The results were compared in Figure 4.19 with the result obtained over untreated catalyst. As can be seen at Figure 4.19, the catalyst lost its performance (yield) approximately 44% if it is used again without any O_2 treatment; both conversion and selectivity decreased. However, if the catalyst was treated with 20% O_2/He at 800 °C during an hour, the performance lost was about 26%. If this catalyst was used as the third time, the performance was decreased to the level of untreated catalyst and further declined after following treatments. This suggests that the O_2 treatment can increase the lifetime of the catalyst initially but there will be still significant activity loss with time.

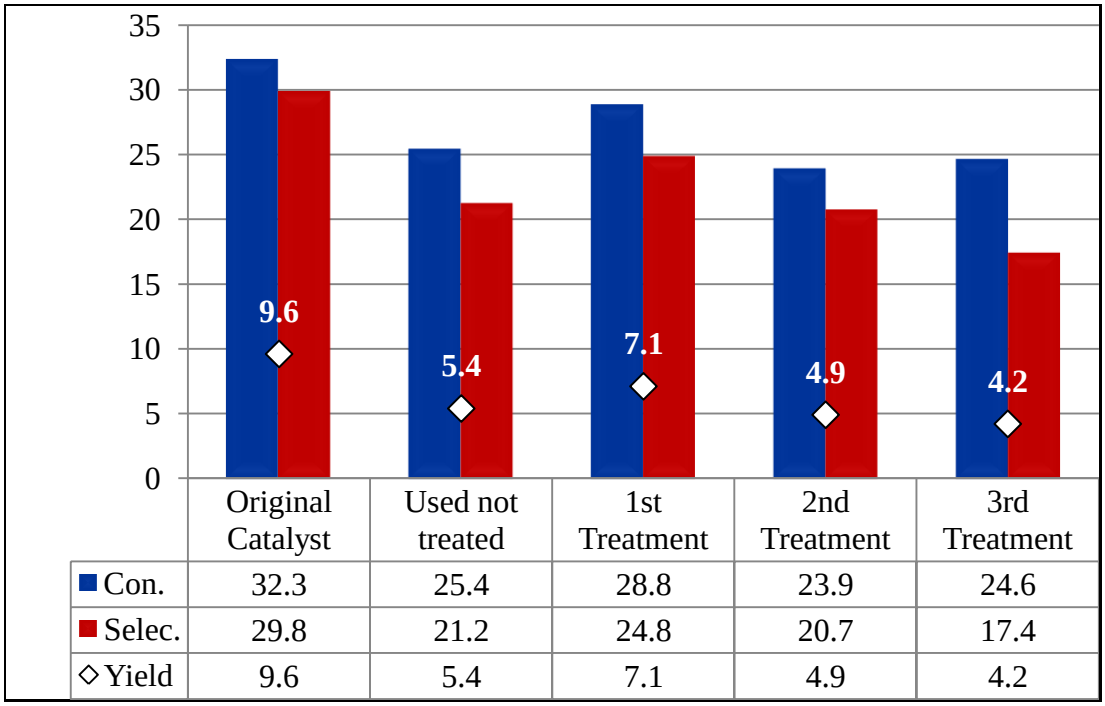

	Original Catalyst	Used not treated	1st Treatment	2nd Treatment	3rd Treatment
Con.	32.3	25.4	28.8	23.9	24.6
Selec.	29.8	21.2	24.8	20.7	17.4
◇Yield	9.6	5.4	7.1	4.9	4.2

Figure 4.19. Investigation for the Recycle Process of Monolites by the Oxygen Treatment Using 10wt.% La_2O_3/10wt.%SrO/MgO Catalyst (Reaction Temperature at 650 °C, CH_4/O_2 ratio is 15).

4.2. Catalyst Characterization

4.2.1. XRD Results

The crystalline phases of the catalyst samples and their particle sizes were identified by using a Rigaku D/MAX-Ultima+/PC X-Ray diffraction equipment having an X-ray generator with Cu target and scan speed of 2 ^{0}/min. The experiments were performed at the Advanced Technologies Research and Development Center of Bogaziçi University.

Figure 4.20 represents the XRD pattern of the unused 10 wt.%La_2O_3 promoted MgO particulate catalyst conforming the La_2O_3 form; the MgO peaks are also obvious. The XRD patterns of 10 wr.% La_2O_3 and 10 wt.% SrO over MgO (Figure 4.21) also shows the corresponding peaks for these oxides, however the MgO peaks do not exist indicating that the surface was fully covered by La_2O_3 and SrO.

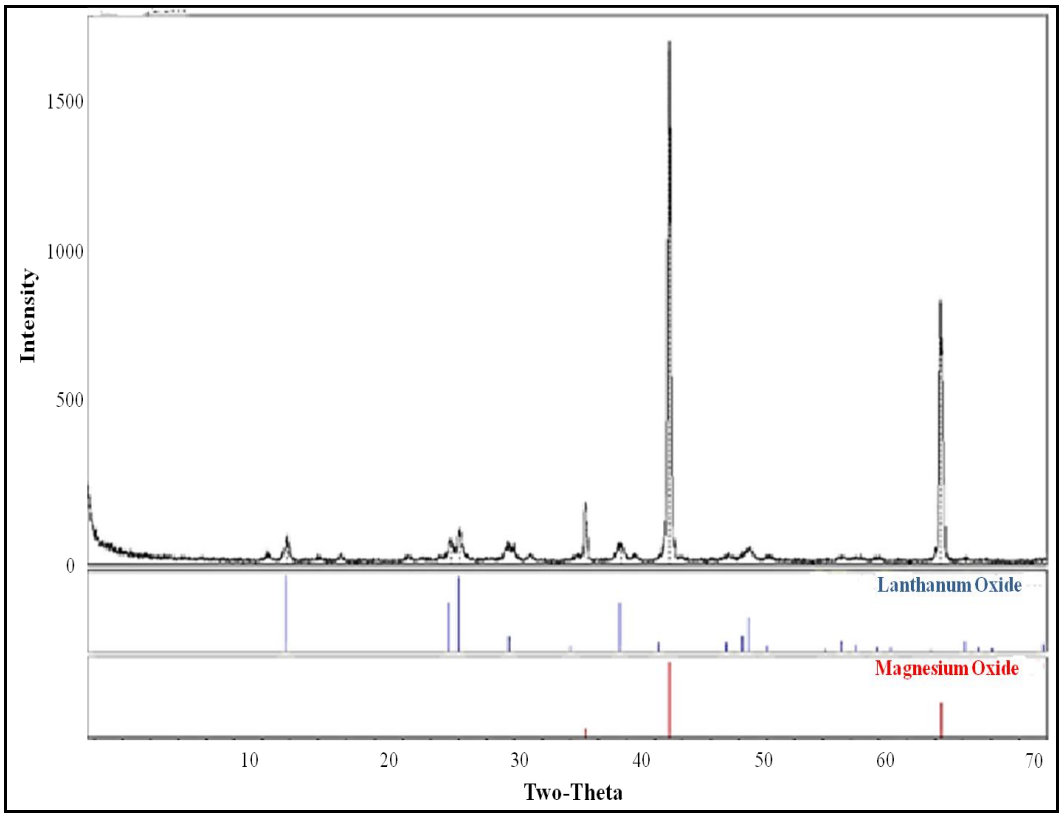

Figure 4.20. XRD Pattern of the Unused La_2O_3 Promoted MgO Particulate Catalyst.

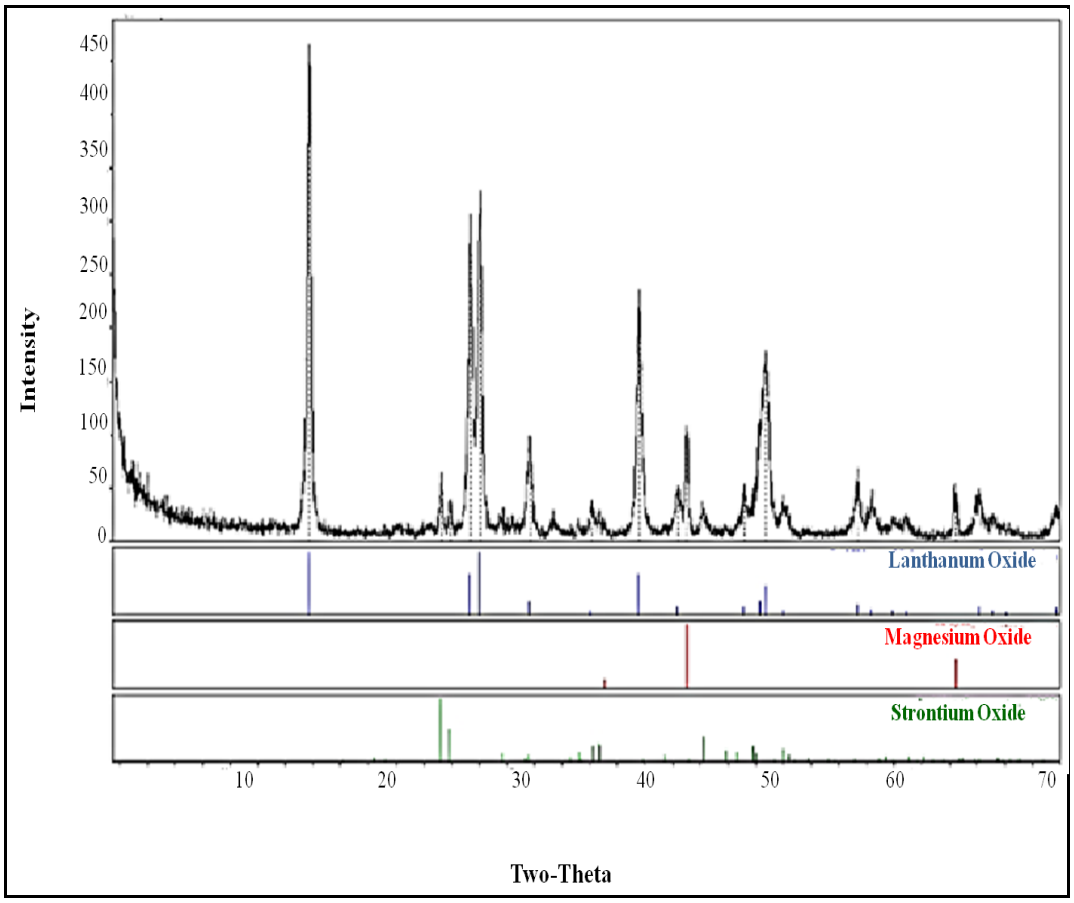

Figure 4.21. XRD Pattern of the Unused La_2O_3 and SrO Promoted MgO Particulate Catalyst.

4.2.2. SEM-XRD Results

Micrographs of the fresh and used catalyst samples as well as the support materials were taken using an environmental scanning electronic microscope (ESEM), to observe the morphological differences. X-ray analytical mapping and Energy Dispersive X-Ray Spectroscopy (EDS) tests were also conducted on catalyst samples in order to clarify their elemental analysis and to obtain information on the dispersion of the metals on the catalyst surface. The tests were conducted in a Philips XL 30 ESEM-FEG system, having a maximum resolution of 2 nm. The experiments were performed at the Advanced Technologies Research and Development Center of Bogaziçi University.

SEM images of 10wt.% La_2O_3/10wt.% SrO /MgO monolith structure are represented in Figure 4.22. (a) show the vertical view of uncoated monolith while (b) represent the horizontal image; (c) and (d) respectively show the vertical and horizontal views of unused monolith coated with 10wt.%La_2O_3/10wt.% SrO/MgO while (d and e) represent the images of used 10wt.%La_2O_3/10wt.%SrO/MgO catalyst. Wall-coating can be easily observed comparing the (a) and (c) at Figure 4.22 and after reaction. It was also clear that the morphology of coating was ion and other physical effects. Figure 4.23 shows the enlarged view of coated part in unused monolithic 10wt.%La_2O_3/10wt.%SrO/MgO.

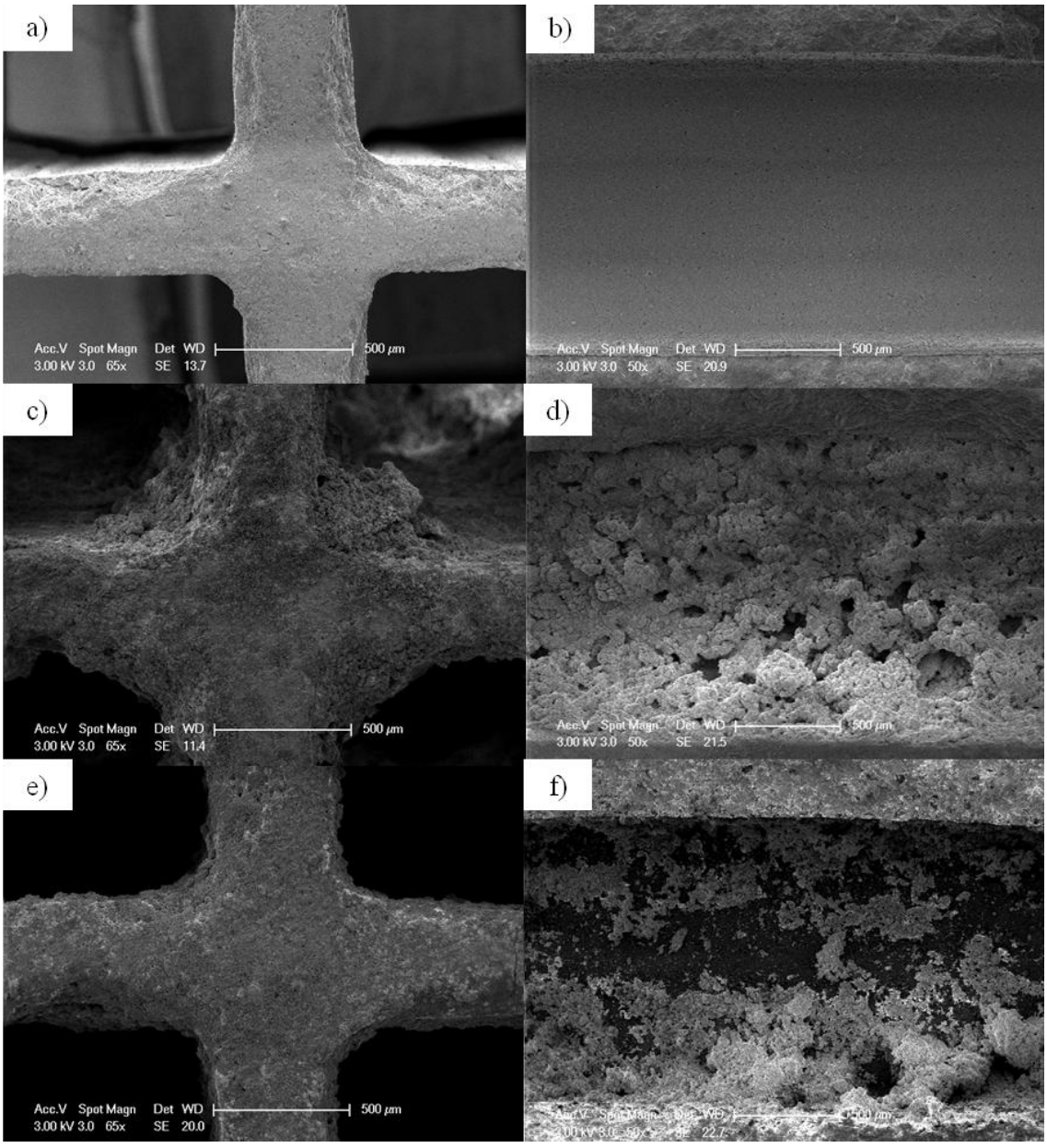

Figure 4.22. SEM Images of 10wt.% La_2O_3/10wt.% SrO/MgO Monolith Structure.

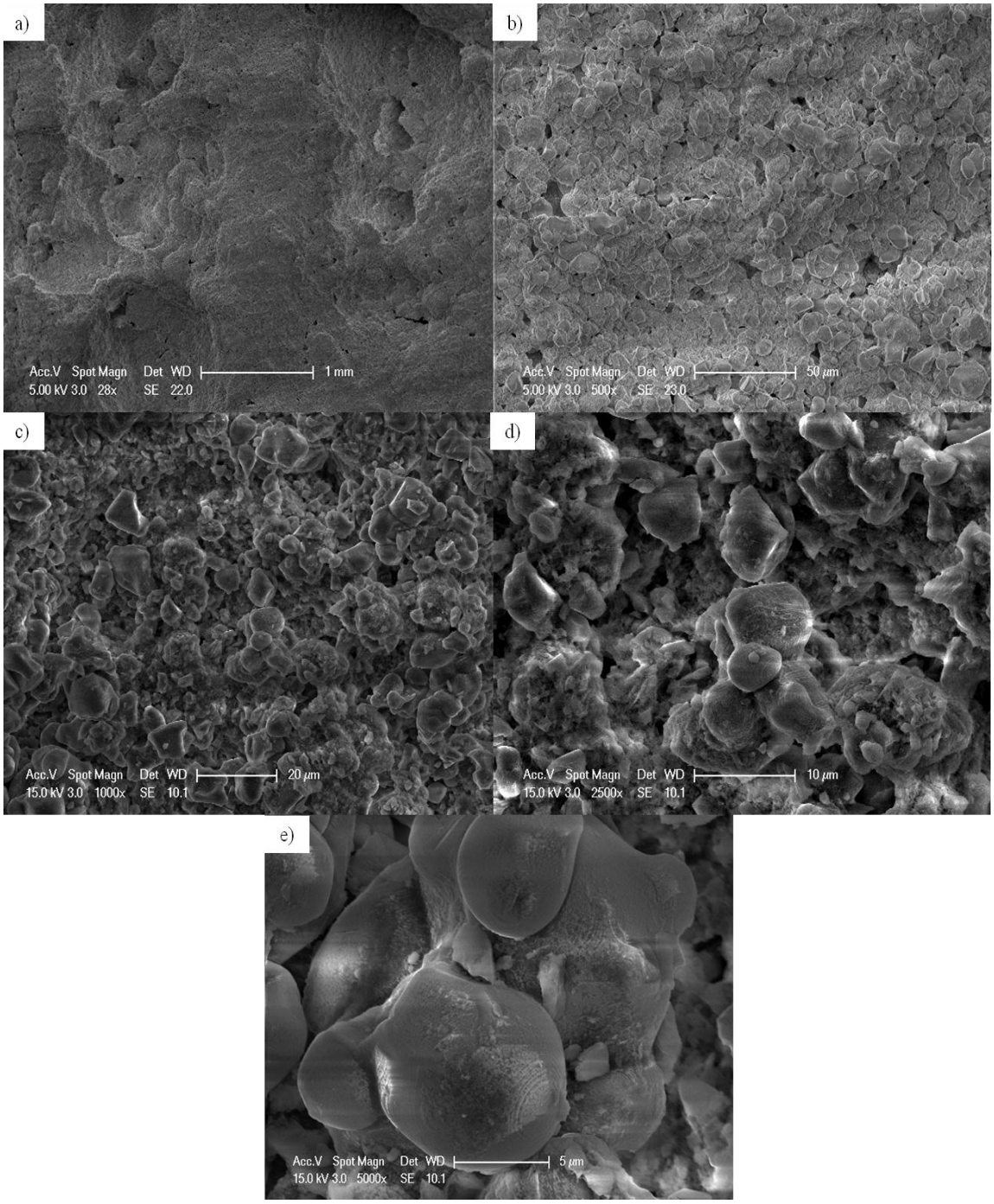

Figure 4.23. SEM Images of 10wt.% La_2O_3/10wt.% SrO/MgO Monolith
(a) 28x, (b) 500x, (c) 1000x, (d) 2500x, (e) 5000x.

SEM and EDX images of unused 10wt.%La_2O_3/10wt.%SrO/MgO particulate catalyst are given in Figure 4.24; (a) is lanthanum, (b) is strontium indicating that both are well dispersed on the magnesium support structure.

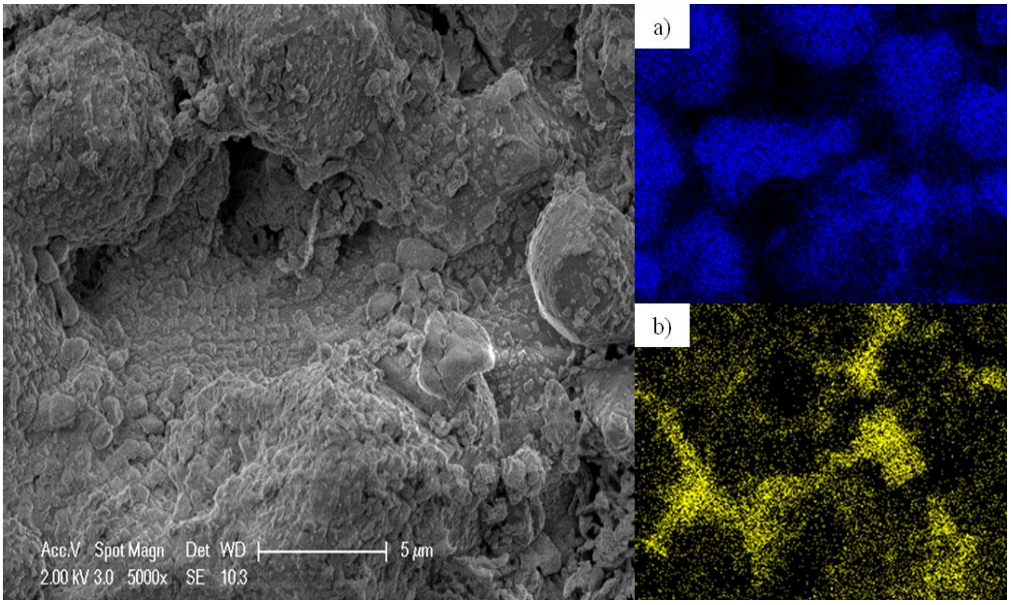

Figure 4.24. SEM (left) and EDX (right) Images of the Unused La_2O_3 and SrO Promoted MgO Particulate Catalyst (a) La, (b) Sr (5000×).

The SEM images of used 10wt.%La_2O_3/10wt.%SrO/MgO particulate catalyst are given in Figure 4.25. The part (a) represents the lanthanum, while (b) represents strontium as the previous figures. The part (c) is for carbon indicating the possible coke formation on catalyst surface during after reaction.

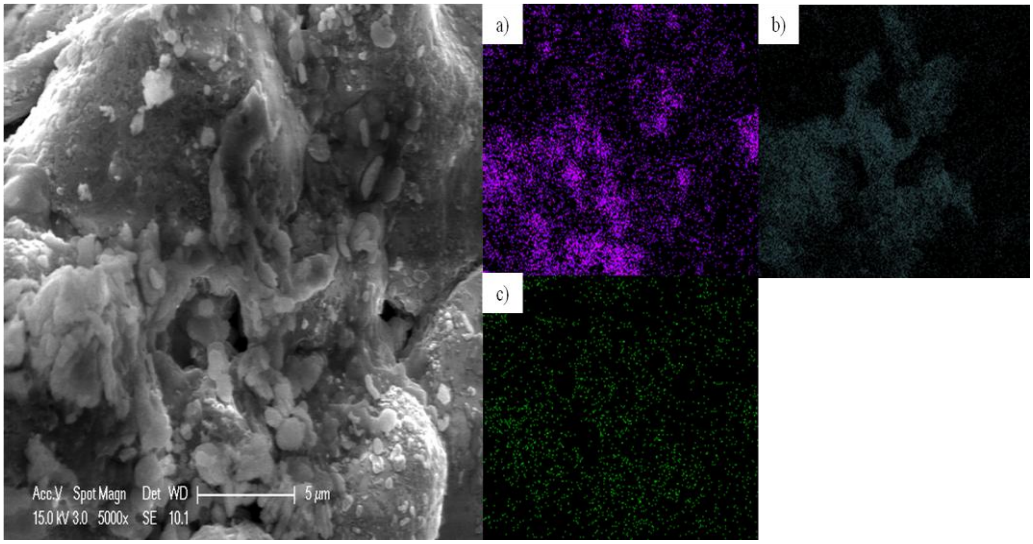

Figure 4.25. SEM (left) and EDX (right) Images of the Used La_2O_3 and SrO Promoted MgO Particulate Catalyst (a) La, (b) Sr, (c) C (5000×).

5. CONCLUSIONS AND RECOMMENDATIONS

5.1. Conclusions

The aim of this study was to investigate the difference between particulate and monolithic catalyst, and the effects of various reaction parameters on the performance of 10wt.%La_2O_3/MgO and 10wt.%SrO/10wt.%La_2O_3/MgO catalysts for OCM reactions.

The prominent conclusions that can be reached from the study are as follows;

- The experiments that conducted to investigate the difference between the particulate and cordierite monolith structure catalyst form show that monolithic form has higher catalytic activity.

- Various catalysts with different metal content were tested to both in the particulate and monolithic form and, 10wt.%SrO/10wt.%La_2O_3/MgO over monolith had highest catalytic activity with 14.5% yield.

- No significant effect of diluent gas on the reaction performance was observed.

- Various CH_4/O_2 molar flow rate ratios were tested and 15/1 was found to be the best for both particulate and monolith catalysts.

- Inside diameter of quartz reactor was decreased 10 mm to 2 mm after the catalyst bed, and this improved both of the C_2 selectivity and the conversion. Filing the empty space in the quartz reactor volume with large size quartz chips or quartz wool also improved the catalystic performance.

- Investigation about the metal loading on SrO/La_2O_3/MgO monolith showed that the 10wt.%SrO/10wt.%La_2O_3/MgO is the best.

- For the the reuse of the catalyst, O_2 treatment was worked in some extend; O_2 trated catalyst had better performance in the second use compared to the untreated catalyst. However this effect gradually dimished in the second and third treatment.

5.2. Recommendations

According to the results of the present study, the following points are thought to be worthwhile for the future studies regarding oxidative coupling of methane over lanthanum and strontium promoted magnesium catalyst:

- In this work, cordierite monolithic structure was prepared according to wall-coating method. Other preparation methods such as wet impregnation, co-precipitation, dry impregnation, deposition-precipitation and homogeneous deposition precipitation can be tried.

- There is limited study on monolith regarding oxidative coupling of methane. More studies can be employed in this field as a plus of other applications of monoliths.

- In this work, 10wt.%SrO/10wt.%La_2O_3/MgO, 20wt.%SrO/10wt.%La_2O_3/MgO and 10wt.%SrO/20wt.%La_2O_3/MgO were studied. Other loadings can be investigated.

- Kinetic experiments of monolithic catalysts can be conducted.

- Different type monoliths have different molecular formula can be tried to investigate catalytic activity.

REFERENCES

Aigler, J. H. and J. H. Lunsford, 1991, "Oxidative Dimerization of Methane Over MgO and Li^+/MgO Monoliths", *Applied Catalysis*, Vol. 70, pp. 29-42.

Amenomiya, Y., V. I. Birss, M. Goledzinowski, J. Galuszka, and A. R. Sanger, 1990, "Conversion of Methane by Oxidative Coupling", *Catalyst Reviews: Science and Engineering*, Vol. 32, pp. 163-227.

Andorf, R., L. Mleczko, D. Schweer, and M. Baerns, 1991, "Oxidative Coupling of Methane in a Bubbling Fluidized Bed Reactor", *The Canadian Journal of Chemical Engineering*, Vol. 69, pp. 891-897.

Arndt, S., G. Laugel, S. Levchenko, R. Horn, M. Baerns, M. Scheffler, R. Schlögl, and R. Schomäcker, 2011, "A Critical Assessment of Li/MgO-Based Catalysts for the Oxidative Coupling of Methane", *Catalysis Reviews: Science and Engineering*, Vol. 53, pp. 424-514.

Baerns, M., D. Schweer, and L. Meeczkol, 1990, "Oxidative Coupling of Methane: Maximizing the Yield of Coupling Products under Co-feed Operating Conditions", *Catalysis Today*, Vol. 6, pp. 453-462.

Bartek J. P., J. M. Hupp, J. F. Brazdil, and R. Grasselli, 1988, "Oxidative Dimerization of Methane over Lead-Magnesium Mixed Oxide Catalysts", *Catalysis Today*, Vol. 3, pp. 117-126.

Borchert, H. and M. Baerns, 1997, "The Effect of the Oxygen-Anion Conductivity of Metal Oxide-Doped Lanthanum Oxide Catalysts on Hydrocarbon Selectivity in the Oxidative Coupling of Methane", *Journal of. Catalysis*, Vol. 168, pp. 315-320.

Bouwmeester, H. J. M., 2003, "Dense Ceramic Membranes for Methane Conversion", *Catalysis Today*, Vol. 82, p. 141.

Burch R., G. D. Squire and S. C. Tsang, 1988, "Comparative Study of Catalysts for the Oxidative Coupling of Methane", *Applied Catalysis*, Vol. 43, p. 105.

Carreiro, J. A. S. P., G. Follmer, L. Lehmann, and M. Baerns, 1988, "Natural Calcium Minerals as Catalyst of Oxidative Conversion of Methane", *Journal of the Chemical Society*, Vol. 2, p. 891.

Carreiro, J. A. S. P, M. Baerns, "Catalytic Conversion of Methane by Oxidative Coupling to C_2 Hydrocarbons", 1987, *Reaction Kinetics and Catalysis Letters*, Vol. 35, No. 1-2, pp. 349-360.

Chen Q., B. Hoebink, and G. B. Marin, 1991, "Effect of Diffusion Limitations of Surface Produced Radicals on the C_2 Selectivity in the Oxidative Coupling of Methane", *Industrial & Engineering Chemistry Research*, Vol. 30, p. 2088.

Choudhary, V. R., S. T. Chaudhari, A. M. Rajput, and V. N. Rane, 1989, "Beneficial Effect of Oxygen Distribution on Methane Conversion and C_2 Selectivity in Oxidative Coupling of Methane to C_2 Hydrocarbon over Lanthanum-Promoted Magnesium Oxide", *Journal of the Chemical Society*, Vol. 32, pp. 1526-1527.

Choudhary V.R., R. Vasant, S. A. R. Mulla, and V. H. Rane, 1998, "Oxidative Coupling of Methane and Oxidative Dehydrogenation of Ethane over Strontium-Promoted Rare Earth Oxide Catalysts", *Journal of Chemical Technology and Biotechnology*, Vol. 71, pp. 167-172.

Choudhary V. R., R. Mulla, and B. S. Uphade, 1999, "Oxidative Coupling of Methane Over Alkaline Earth Oxides Deposited on Commercial Support Precoated with Rare Earth Oxides", *Fuels*, Vol. 78, pp. 427-437.

Choudhary, V. R., V. H. Raneh, and S. T. Chaudhari, 2004, "Oxidative Coupling of Methane over La-promoted MgO catalysts: Influence of Precursors and Method of Catalyst Preparation", *Indian Journal of Chemical Technology*, Vol. 2, pp. 569-574.

Choudhary V. R. and B. S. Uphade, 2004, "Oxidative Conversion of Methane/Natural Gas Into Higher Hydrocarbons", *Catalysis Surveys from Asia*, Vol. 8, pp. 15-25.

Dry M.E., 2002, "The Fischer-Tropsch Process: 1950-2000", *Catalysis Today*, Vol. 71, p. 227.

Düşova, Y., 2014, *An Experimental Study on Oxidative Coupling of Methane over $Mn/Na_2WO_4/SiO_2$ Catalyst*, M. Sc. Thesis, Bogazici University, Istanbul.

Frade, J. R., V. V. Kharton, A. Yaremchenko, and E. Naumovich, 1997, "Methane to Syngas Conversion. Part I. Equilibrium Conditions and Stability Requirements of Membrane Materials", *Journal of Power Sources*, Vol. 130, p. 77.

Fujimoto K., H. E. Curry-Hyde, and R. F. Howe, 1994, "Natural Gas Conversion Proceedings of the Third Natural Gas Conversion", *Studies in Surface Science and Catalysis*, Vol. 81, p. 73.

Fujimoto, K., S. Hashimoto, K. Asami, and H. Tominaga, 1987, "Selective Oxidative Coupling of Methane Catalysed over Hydroxyapatite Ion-Exchanged with Lead", *Chemistry Letters*, Vol. 2157, p. 58.

Gao, Z. and Y. Shi, 2010, "Suppressed Formation of CO_2 and H_2O in the Oxidative Coupling of Methane over La_2O_3/MgO Catalyst by Surface Modification", *Journal of Natural Gas Chemistry*, Vol.19, pp. 173–178.

Ghiasi M., A. Malekzadeh, S. Hoseini, Y. Mortazavi, A. Khodadadi, and A. Talebizadeh, 2011, "Kinetic Study of Oxidative Coupling of Methane over Mn and/or W promoted Na_2SO_4/SiO_2 catalysts", *Journal of Natural Gas*, Vol. 20, pp. 428-434.

Hinsen, W., W. Bytyn, and M. Baerns, 1984, "Oxidative Dehydrogenation and Coupling of Methane", Proceedings of the 8th International Congress on Catalyst, Berlin.

Ito, T., and J. H. Lunsford, 1985, "Catalytic Conversion of Methane to Methanol, Formaldehyde and Higher Hydrocarbons", *Nature,* Vol. 314**,** p. 721.

Iwamatsu E., T. Moriyama, N. Takasaki, and K. Aika, 1987, "Oxidative Coupling of Methane over Alkali-Doped Antimony Oxide", *Journal of Chemical Education*, Vol. 19. pp. 56-59.

Jähnisch, K., V. Hessel, H. Löwe, and M. Baerns, 2004, "Chemistry in Microstructured Reactors", *Angewandte Chemie International*, Vol. 43, pp. 406-446.

Jones, C.A., J. J. Leonard, and I. A. Sofianko, 1987, "The Oxidative Conversion of Methane to Higher Hydrocarbons over Alkali-Promoted $Mn/Si0_2$", *Journal of Catalysis*, Vol. 103, pp. 311-319.

Keller, G. E. and M. M. Bhasin, 1982, "Synthesis of Ethylene via Oxidative Coupling of Methane: I. Determination of Active Catalysts", *Journal of. Catalysis,* Vol. 73, pp. 9-19.

Kim, S. C., L. E. Erickson, and E. Y. Yu, 1995, "Reducing the Formation of Carbon Oxides in the Production of C_{2+} Hydrocarbons from Methane", *Journal of Hazardous Materials*, Vol. 41, pp. 327-340.

Kolb, G. and V. Hessel, 2004, "Review of Micro-Structured Reactors for Gas Phase Reactions", *Chemical Engineering Journal*, Vol. 98, pp. 1-38.

Labinger J. A. and K. C. Ott, 1990, "Is There a Difference Between Surface and Bulk Oxidation Levels in Partially Reduced Metal Oxides Catalyst?", *Catalyst Letter*, Vol. 4, pp. 245-250.

Lin, C.H., J. X. Wang, and J. H. Lunsford, 1988, "Oxidative Dimerization of Methane Over Sodium Promoted Calcium Oxide", *Journal of Catalysis,* Vol. 111, pp. 302-316.

Lunsford, J. H., 2000, “Catalytic Conversion of Methane to More Useful Chemicals and Fuels: A Challenge for the 21st Century”, *Catalysis Today*, Vol. 63, pp. 165-174.

Machida K. and M. Enyo, 1987, “Oxidative Dimerization of Methane Over Cerium Mixed Oxides and Its Relation with Their Ion-Conducting Characteristics”, *Journal of the Chemical Society*, Vol. 21, pp. 1639-1640.

Marino, F. and M. Duprez, 2005, “Supported Base Metal Catalysts for the Preferential Oxidation of Carbon Monoxide in the Presence of Excess Hydrogen (PROX)”, *Applied Catalysis B: Environmental*, Vol. 58, pp. 175-183.

Mleczko L. and M. Baerns, 1995, “Catalytic Oxidative Coupling of Methane-Reaction Engineering Aspects and Process Schemes”, *Fuel Processing Technology* , Vol. 42 pp. 217-248.

Moulijn, J. A. and A. Cybulski, 2006, *Structured Catalysts and Reactors*, Second Edition, CRC Press, Taylor&Francis Group, Boca Raton, Florida, USA, p. 243.

Olivier, L., S. Haag, C. Mirodatos, and A. Veen, 2009, “Oxidative Coupling of Methane Using Catalyst Modified Dense Perovskite Membrane Reactors”, *Catalysis Today*, Vol. 142, pp. 34-41.

Otsuka, K., Q. Liu, and A. Morikawa, 1986, "Selective Synthesis of Ethylene by Partial Oxidation of Methane over LiCl-Sm_2O_3," *Journal of the Chemical Society Communications*, Vol. 145, pp. 586-587.

Ozdemir, S., 2009, *Selective CO Oxidation Over Monolithic Au/Al_2O_3 Promoted by Metal Oxides*, M. S. Thesis, Bogaziçi University, Istanbul.

Pérez-Cadenas, A. F., M. M. P. Zieverink, F. Kapteijn, and J. A. Moulijin, 2005, “High Performance Monolithic Catalysts for Hydrogenation Reactions”, *Catalysis Today*, Vol. 105, pp. 623-628.

Phillips, C. H., G. Lauschke, and H. Peerhossaini, 1997, "Intensification of Batch Chemical Processes by Using Integrated Chemical Reactor-Heat Exchangers," *Applied Thermal Engineering*, Vol. 17, pp. 809-824.

Pyatnitskii Y. I., 2003, *Theoretical and Experimental Chemistry*, Springer Science Business, Vol. 39, New York, USA.

Rane, V. H., S. T. Chaudhari, and V. R. Choudhary, 2010, "Oxidative Coupling of Methane over La-Promoted CaO Catalysts: Influence of Precursors and Catalyst Preparation Method", *Journal of Natural Gas Chemistry*, Vol. 19, pp. 25-30.

Renken, A. and K. M. Lioubov, 2005, "Microstructured Reactors for Catalytic Reactions", *Catalysis Today*, Vol. 110, pp. 2-14.

Rozovskii A. Y., Y. B. Kagan, G. Lin, E. V. Slivinskii, S. M. Loktev, L. G. Liberov, and A. N. Bashkirov, 1975, "Theoretical Grounds of the Process of Methanol Synthesis", *Kinetic Catalyst*, Vol. 16, p.809.

Sekine, Y., K. Tanaka, M. Matsukata, and E. Kikuchi, 2009, "Oxidative Coupling of Methane on Fe-Doped La_2O_3 Catalyst", *Energy & Fuels*, Vol. 23, pp. 613–616.

Simsek, E., 2012, *Catalytic Synthesis Gas Production in Microchannel Reactors*, Ph.D. Thesis, Bogaziçi University, Istanbul.

Stankiewicz, A. I. and J. A. Moulijn, 2000, "Process Intensification: Transforming Chemical Engineering", *Chemical Engineering Progress*, Vol. 96, pp. 22-33.

Talebizadeh, A., M. Daneshpayeh, A. Khodadadi, N. Mostoufi, Y. Mortazavi, and R. Gharebagh, 2009, "Kinetic Modeling of Oxidative Coupling of Methane Over $Mn/Na_2WO_4/SiO_2$ Catalyst", *Fuel Processing Technology*, Vol. 90, pp. 403-410.

Tan, X., P. Zhaobao, G. Zi, and S. Liu, 2007, "Catalytic Perovskite Hollow Fibre Membrane Reactors for Methane Oxidative Coupling", *Journal of Membrane Science,* Vol. 302, pp. 109-114.

Tomašić, V. and F. Jovic, 2006, "State-of-the-art in the Monolithic Catalysts/Reactors", *Applied Catalysis A: General,* Vol. 311, pp. 112-121.

Uysal, G., 2005, *Effect of Carbon Dioxide and Water Vapor on Selective Carbon Monoxide Oxidation Over Pt Based Catalysts*, M. Sc. Thesis, Bogaziçi University, Istanbul.

Veser, G., 2001, "Experimental and Theoretical Investigation of H_2 Oxidation in a High Temperature Catalytic Microreactor", *Chemical Engineering Science,* Vol. 56, pp. 1265-1273.

Wolf E. E., 1992, *Methane Conversion by Oxidative Processes*, Van Nostrand Reinhold Catalysis Series, New York, USA, pp. 99-137.

Wörz, O., K. P. Jäckel, T. Richter, and A. Wolf, 2001, "Microreactors - A New Efficient Tool for Reactor Development", *Chemical Engineering & Technology*, Vol. 24, p.138.

Yu, L., W. Li, V. Ducarme, C. Mirodatos, and G. A. Martin, 1997, "Oxidative Coupling of Methane and Oxidative Dehydrogenation of Ethane over Strontium-Promoted Rare Earth Oxide Catalysts", *Journal of Chemical Technology and Biotechnology,* Vol. 71, pp. 167-172.

Zanthoff, H.W., 1991, *Oxidative Methankupplung in der Gas-phase,* Ph.D. Thesis, Ruhr-University, Bochum.

Zhu, J., J. Ommen, and L. Lefferts, 2004, "Reaction Scheme of Partial Oxidation of Methane to Synthesis Gas over Yttrium-stabilized Zirconia", *Journal of Catalysis*, pp. 388-398.